The Influence of Colloidal Kaolinite on Th(IV) Transport

in Saturated Porous Media

By

Hangping Zheng

A Thesis Submitted to the Graduate Faculty of
Auburn University
in partial fulfillment of the
requirement for the Degree of
Master of Science

Auburn, Alabama
December 14, 2013

Keywords: Actinide, Thorium(IV), Kaolinite, Porous media,
Colloid-facilitated transport, Colloid-associated retardation

Approved by

Mark O. Barnett, Chair, Malcolm Pirnie Professor of Civil Engineering
Clifford R. Lange, Associate Professor of Civil Engineering
Jose G. Vasconcelos, Assistant Professor of Civil Engineering

Abstract

Many laboratory and field studies have indicated that colloid mobilization was the most important potential source of enhancing the transport of a variety of contaminants in groundwater. However, limited research studied the possibility of colloid-associated retardation. Therefore, this thesis is to investigate the influence of colloidal kaolinite on the migration of Th(IV) (an analog for Pu(IV)) in saturated porous media, including both facilitation and retardation effects. Column experiments were conducted under constant conditions of 0.001 M ionic strength, a pH of 4.0, and specific discharge of 0.2 cm/min.

When 100 mg/L colloidal kaolinite was pumped through uncontaminated quartz sands, it took approximately one pore volume (PV) to break through, and reached to maximum C/C_0 of 0.91 attributed to small and irreversible deposition of colloids onto solid phase by physical-chemical collection between kaolinite colloids and sand particles. The transport of kaolinite was much similar to that of the conservative tracer bromides, indicating high mobility of stable colloids. In contrast, Th(IV) transport showed a significant retardation in colloid-free columns, and the desorption of the actinide was a prolonged, gradual decreasing process. The breakthrough of 1.0 mg/L Th(IV) (20 PVs) required twice as many pore volumes as the 2.65 mg/L Th(IV) transport (10 PVs), and based on mass balance, very close amount of Th(IV) (5mg/kg and 5.7 mg/kg) retained in columns, suggesting that there exists maximum sorption sites on sand surfaces for Th(IV).

The transport of 1 mg/L Th(IV) adsorbed onto 100 mg/L kaolinite exhibited no retardation, but 2.65 mg/L Th(IV) co-transporting with colloids was completely retained in the column. Therefore, the conclusion that kaolinite plays an important role in accelerating transport of Th(IV) is effective only under the condition that Th(IV) and colloidal kaolinite formed mobile pseudo-colloids or the amount of actinides was not enough to destabilize colloids. However, once colloids and actinides transport separately, both mobilities were reduced in different extent due to surface complexation reaction. The kaolinite transport in sand media containing 6.5 or 9.3 mg/kg Th(IV) showed more than 10 times retardation compared to its transport on non-Th(IV) conditions. Furthermore, no increase of Th(IV) concentration was observed when kaolinite broke through and increased, indicating that kaolinite failed to stripe Th(IV) off the sand matrix to enhance the contaminant transport. Whereas 1 mg/L and 2.65 mg/L of Th(IV) mobilization triggered a release of about 38% and 45% kaolinite entrapped in pore constrictions due to physical-chemical forces. Moreover, both initial breakthroughs of 1 mg/L and 2.65 mg/L Th(IV) movement were delayed approximately twice in the column containing 302 mg/kg kaolinite with 5 mg/kg Th(IV) and 340 mg/kg kaolinite with 6 mg/kg Th(IV) compared to both transports in the absence of colloids. Hence, kaolinite deposition onto sand media could increase retention of Th(IV) transport attributed to increasing the accessibility of adsorption sites for Th(IV).

Acknowledgments

The author would like to express her gratitude for the wonderful guidance and support of her advisor, Dr. Mark Barnett. The author would also like to thank her other committee members, Dr. Clifford R. Lange and Dr. Jose G. Vasconcelos, and the rest of the environmental faculty in the Civil Engineering department for their instruction, knowledge, and support during the author's time at Auburn University. Furthermore, the author would like to thank Jinling Zhuang for his technical assistance and support in the environmental laboratory. The author would especially like to thank Daniel Gingerich for his help with thesis revisions. Finally, I would like to thank my husband, family, and friends who supported me throughout my studies here at Auburn University.

Table of Contents

List of Tables

List of Figures

Chapter One

Introduction

1.1 Problem statement

Radioactive waste has been an important environmental concern for several decades, because a substantial amount of actinides used in nuclear weapon programs and nuclear power production have accumulated as waste since the 1940s (Ahearne 1997). Due to improper nuclear operation and storage, a large amount of actinides has been spilled into groundwater, contaminating aquifer systems (Ahearne 1997; Runde 2000). For example, there are several critical sites where plutonium (Pu) have been released into the environment including the Los Alamos National Laboratory, Nevada Test Site, Savannah River Site, Maxey Flats in Kentucky, and Mayak Production Association in Russia (Cantrell and Riley 2008). In addition to these environmental incidents, radioactive waste disposal in geologic repositories might also eventually result in significant amounts of nuclear waste leaking into groundwater, because waste containers will probably be corroded before the actinides decay completely, which takes tens of thousands of years (Melson 2012; Runde 2000). Therefore, the study of chemical interactions between the actinides and the environment and their transport in aquifer systems is needed to understand and prevent contaminants migrating through the groundwater.

Actinides, which have electrons that fill the 5f orbitals, exhibit multiple oxidation states and are capable of forming many different molecular species (Runde 2000). There are several chemical interactions actinides undergoing in the environment, including oxidation-reduction (redox), complexation, transport, dissolution-precipitation, sorption and bioavailability (Runde 2000). Which chemical reaction is predominant depends on the properties of the local conditions, such as temperature, water pH, pressure profiles, redox potential, and ligands concentration (Runde 2000). Tetravalent actinide ions (An(IV)) readily hydrolyze to form the strongest and most stable complexes in aquatic systems, while the ability of pentavalent actinide ions (An(V)) to form complexes is weakest. In other words, An(IV) species have a strong tendency to adsorb onto rock or mineral surfaces and have low solubility in groundwater (Neck and Kim 2001; Runde 2000). Due to the low concentration and strong affinity for the solid phase, actinides were originally expected to be immobile in porous media (Kersting et al. 1999). However, some field studies have reported that actinides have been detected long distances from their source areas (Cantrell and Riley 2008; Kaplan et al. 1994; Kersting et al. 1999; Penrose et al. 1990). There are a number of possibilities for causing actinides mobilization in the subsurface, but colloidal-facilitated transport has been implicated as the major reason for this unexpected long-distant migration of contaminants.

Colloidal particles, widely distributed in groundwater systems, have high specific surface areas typically ranging from 10 to 800 $m^2 g^{-1}$ due to their small sizes (1 nm to 1 μm) (Kersting et al. 1999). In the natural aqueous environment, most mobile colloids consist of clay minerals such as kaolinite or illite, mineral precipitates such as ferric oxides or ferric hydroxides, organic biopolymers such as humic or fulvic acids, and

biocolloids like viruses or bacteria (Kretzschmar and Schafer 2005). Under some specific conditions, significant quantities of colloids can be released from the solid aquifer matrix by changes in flow velocity, water saturation, and solution chemistry (Kretzschmar and Schafer 2005; Ryan and Elimelech 1996; Sen and Khilar 2006). Chemical perturbation was the chief mechanism for colloids release, such as decreases in ionic strength, increases in pH, or adsorption of solutes (Burgisser et al. 1993; Grolimund 2005; McCarthy and Zachara 1989; Ryan and Elimelech 1996; Sardin et al. 1991). Once colloids are free, they can migrate by advection and dispersion or may redeposit due to mass transfer reactions that happen at the mineral-grain surface and the air-water interface (Saiers and Lenhart 2003). Most importantly, the contaminants adsorbed strongly by colloids may transport simultaneously in natural porous media and eventually enter into the groundwater aquifers, negatively affecting the quality of drinking water (McGechan and Lewis 2002; Ryan et al. 1998; Sprague et al. 2000). Some studies have indicated that inorganic colloids were primarily responsible for the migration of transition metals and actinides in soils and aquifers (Ryan and Elimelech 1996). Moreover, it is easier and faster for quartz and kaolinite to release from the soil matrix than other colloids during changes in chemical or physical conditions, like decreasing ionic strength, increasing pH or enhancing flow rate (Kaplan et al. 1993). Therefore, kaolinite has been used as a clay colloid in many laboratory column transport experiments to study the transport of heavy metals or actinides in porous media (Ryan and Elimelech 1996).

At many Department of Energy sites, Pu has been detected migrated away from the sources (Cantrell and Riley 2008). For examples, trace Pu was detected in groundwater 1.3 km from Nevada Test site. However, it is extremely difficult to study Pu

in the laboratory because its III, IV, and V oxidation states can co-exist in the normal range of natural waters (Choppin 2007; Runde 2000). Fortunately, Pu(IV) is the most prevalent oxidation state in most subsurface environments, and actinides in the same oxidation state tend to behave similarly (Choppin 1999; Guo et al. 2005; Hongxia et al. 2007; Hongxia et al. 2006). Consequently, thorium (Th(IV)) which exists only in one oxidation state in the environment may be used as an analog for Pu(IV) to study whether inorganic colloid transport is the key to facilitate the migration of tetravalent actinides (Choppin 2007). There is a significant body of literature on the colloid-facilitated transport of contaminants, but limited research examined colloid-associated transport of actinides including both facilitation and retardation influence.

1.2 Objective

The primary objectives of this thesis were (1) to determine the transport of colloidal kaolinite and Th(IV) in saturated porous media, (2) to investigate colloid-facilitated transport and its effect on Th(IV) migration by comparing the transport behavior of colloidal Th(IV) (Th(IV) adsorbed onto kaolinite before transport) and soluble Th(IV), (3) to test whether kaolinite can scavenge Th(IV) adsorbed onto sand media, and (4) to examine the possibility of colloid-associated retardation of contaminants by comparing Th(IV) transport in sand columns with and without kaolinite present.

1.3 Organization

The organization of this thesis follows the guidelines for a publication-style thesis as outlined in the *Guide to Preparation and Submission of Theses and Dissertations* by

the Auburn University Graduate School. There are four chapters in the thesis. Chapter One is an introduction including the problem statement and objectives of this research. Chapter Two is a literature review presenting in-depth background information. The materials, methods, and results from the experiments are discussed in Chapter Three. This chapter is formatted as a draft manuscript, which will be submitted later for publication in a peer-reviewed scientific journal. Chapter Four contains the conclusions from this study, as well as recommendations for future work.

Chapter Two

Literature Review

2.1 Radioactive Waste and Contamination

Radioactive waste has been a significant environmental concern over the past seventy years since substantial amount of radioactive materials were produced in the nuclear weapon programs and nuclear power industries. The inventory of transuranics, including neptunium (Np), plutonium (Pu), americium (Am), and curium (Cm), has been enhanced remarkably from 1942, when the first fission reactor built to 1990 (Runde 2000). Most of them have accumulated as waste worldwide, and the U.S. alone has millions of cubic meters and tens of billions of curies of radioactive waste (Ahearne 1997). For instance, the combined volume of high-level waste (HLW), low-level waste (LLW) and transuranic (TRU) waste from both commercial and government operations was about 5.5 million cubic meters and the radioactivity of all anthropogenic sources was about 31 billion curies by the end of 1995 (Ahearne 1997).

Nowadays, storing aboveground in the interim storage facilities is the primary method to isolate most spent nuclear fuel. However, scientists and government agencies in the United States and some European countries have been seeking final disposal methods for radioactive waste for over twenty years because of the space limitations to store additional fuel. One of the proposed solutions is to build nuclear waste repositories

deep underground to deposit the radioactive waste for at least tens of thousands of years, which is necessary given the actinides' long half life (Kim et al. 2011; Runde 2000). However, it is possible that waste containers will deteriorated by water seeping into a repository before the radionuclides decay sufficiently, potentially causing leakages of nuclear wastes into the soil and eventually leading to environmental contamination (Melson 2012; Runde 2000).

When researchers conducted underground nuclear tests around detonation sites, they found that most radioactive elements are immobile, except Pu which was discovered at the Nevada Test Site more than one kilometer away (Cantrell and Riley 2008; Runde 2000). Long-distant migration of Pu has been noted at four other waste sites (Cantrell and Riley 2008). The reason for the unanticipated migration of Pu inferred by many scientists is colloid-facilitated transport. Nevertheless, there was no direct evidence to prove that colloid-facilitated transport is the major factor resulting in enhanced transport of Pu in these cases (Cantrell and Riley 2008). Hence, it is very critical to study which factors control or influence the transport of radioactive waste migrating through the groundwater. Such information can help not only to assess the risk posed by a contaminant to human health but also to develop and evaluate plans for cleaning contaminated waste sites.

2.2 Actinides and the Environment

Actinides are located in the last row of the periodic table involving 15 metallic chemical elements from actinium (atomic number 89) to lawrencium (atomic number 103) (Table 2.1). Of the actinides, thorium (Th), uranium (U) and protactinium (Pa) occur naturally, while other elements are decay products from uranium, created from uranium reactions or artificially synthesized (Seaborg and Loveland 1990). In addition, six

actinide elements are of long-term environmental concerns including thorium, uranium, neptunium, plutonium, americium and curium (Clark et al. 1995). Due to electrons filling in the 5f orbitals, many actinides show multiple oxidation states and are capable of forming lots of distinct molecular species (Runde 2000). Moreover, the same element in different oxidation states can exist simultaneously in the same solution, such as U, Np, and especially Pu (which can display four oxidation states even in a simple aqueous system) (Clark et al. 1995; Runde 2000). These multiple oxidation states complicate the chemical interactions of actinides in environmental systems. However, some of the actinides such as Am(III), Cm(III), and Th(IV) prefer to be present in one oxidation state in the environment (Choppin 2007). Furthermore, actinides in the same oxidation state have similar chemical behavior (Runde 2000). Therefore, analogs have been used to study the behavior of complex actinides, such as Am(III) substituting for Pu(III) and Th(IV) replacing Pu(IV) (Choppin 2007; Haliena 2012).

Table 2.1: Periodic Table of the Elements. Copied from About.Com Chemistry (2013).

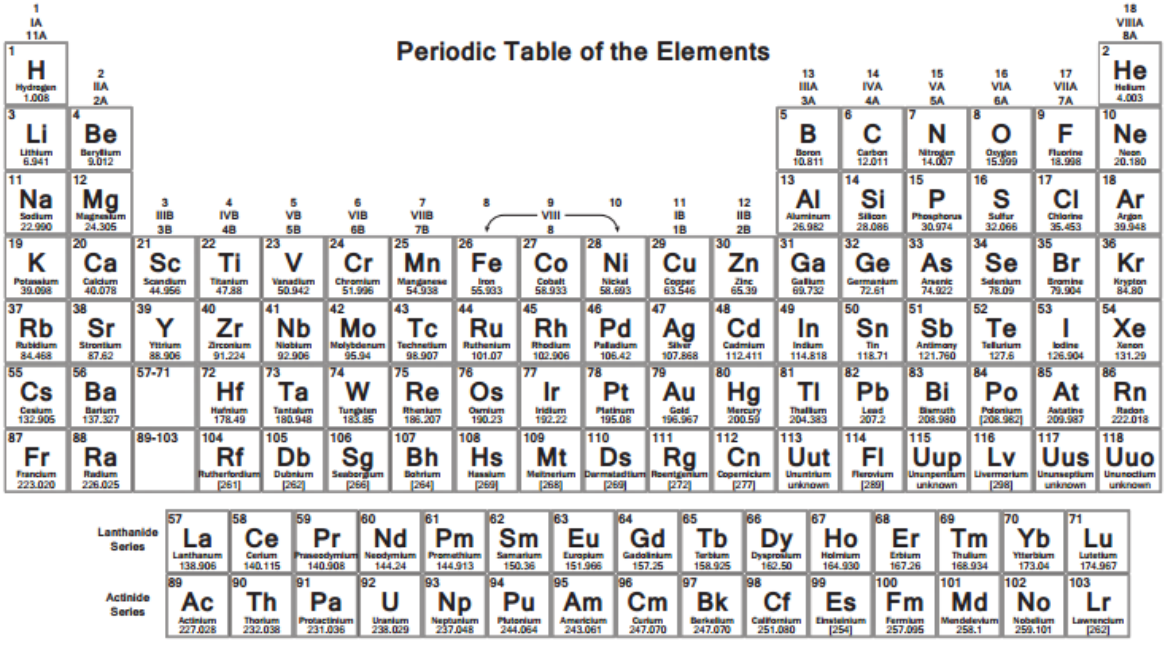

Although the dynamic interaction between the actinides and the environment is complicated, there are six dominant behaviors of actinides in the subsurface: dissolution and precipitation, sorption, transportation, complexation, oxidation-reduction, and bioavailability (Runde 2000). The upper actinide concentration in solution is determined by precipitation and dissolution, while sorption onto soil or colloids influences actinide immobilization and transport (Choppin 2007; Runde 2000).

2.3 Thorium (IV) as an Analog for Plutonium (IV)

Of the actinides**,** plutonium is of the most significant environmental concern because of its deep migration in the environment. Reports showed that five out of seven waste sites (Los Alamos National Laboratory; Nevada Test Site; Savannah River Site; Maxey Flats at Kentucky; Mayak Production Association in Russia) have detected Pu in aqueous systems far away from the sources (Cantrell and Riley 2008). For example, trace Pu was detected in groundwater 4 kilometers from the point of waste discharge at the Mayak Production Association in Russia (Cantrell and Riley 2008). To study how plutonium transports through the subsurface, the local conditions are important including temperature, pressure profiles, pH, redox potential (Eh), and ligand concentration, in addition to the intricate interplay between the actinide and the environment (Runde 2000). Due to its various oxidation states and many severe health hazards (e.g., kidney damage), many researchers use other actinide elements to simulate the behavior of plutonium in groundwater (EPA 2012).

Based on the effective charges of the ion, tetravalent actinides form the strongest and most stable complexes, so Pu(IV) was expected to be the predominant oxidation state in most ocean or groundwater environments (Runde 2000). In general, Th(IV) has been

thought the ideal oxidation state analog for Pu(IV), though the complexation of Th(IV) is somewhat weaker and tends to hydrolyze more readily (Choppin 1999). Therefore, when using Th(IV) as a model for Pu(IV) behavior, some corrections and adjustments based on the difference in the atomic radii are required (Choppin 1999).

2.4 General Thorium Mineralogy, Chemistry, and Toxicology

Thorium is a soft, ductile, and radioactive metal that occurs naturally at low concentrations in soil, rock, water, plants, and animals, at about 6 parts per million (mg/kg) in soil (ATSDR 1990; Peterson et al. 2007). Monazite sands ($ThPO_4$), containing 3 to 10% of thorium oxide, are the chief source of thorium present in the environment, whereas the mineral thorite ($ThSiO_4$) and thorianite (ThO_2) also can provide small amounts of thorium (Freidman 2011; Peterson et al. 2007). Thorium has a very strong affinity to soil particles, especially clay soil, which causes thorium to be less mobile with concentrations in soil more than 5000 times higher than in interstitial water (Peterson et al. 2007).

A silvery-white heavy metal, thorium has a similar density to lead, and it glows with a white light when heated in air (which is why thorium has been used to make lantern mantles) (EPA 2011; Peterson et al. 2007). It also can be used as a fuel for creating nuclear energy (ATSDR 1990). There are 26 known isotopes of thorium, but most natural thorium (99%) is in the isotope form of thorium-232, which has a radioactive half-life of fourteen billion years (ATSDR 1990; Peterson et al. 2007). Thorium-232 slowly decays by alpha emission, with accompanying gamma radiation to form radium-228 until stable lead-208 is created (EPA 2011).

Thorium was ranked at 102 in the 2011 Priority List of Hazardous Substances by the Agency for Toxic Substances and Disease Registry (ATSDR) (ATSDR 2011). Studies have shown that exposure to thorium may increase the chance to develop lung or pancreatic cancer, and bone cancer is another potential cancer (ATSDR 1990). Blood disorders and liver tumors are the two primary health effects for people injected with high doses of thorium (Peterson et al. 2007). To cause the above diseases, thorium has to enter the body first because the amount of gamma radiation emitting from thorium was very small. The main pathways of thorium into the body are inhalation of dust containing thorium and ingestion of food and water contaminated with thorium (Peterson et al. 2007). The limitation for gross alpha particle activity in drinking water set by EPA is 15 pCi/L, equivalent to 136 μg/L of thorium (ATSDR 1990; Haliena 2012).

2.5 Aqueous Speciation of Th(IV)

In an aqueous system, metal ions have a strong tendency to complex anions or ligands existing in the solution. These chemical species (the speciation of the metal ion) describe the distribution of the metal ion in a system. It is extremely important to understand the speciation of an element in order to analyze the behavior of a contaminant in the environment, since solubility, toxicity, and adsorption onto soil particles all depend on speciation (Haliena 2012; Melson 2012). Hydroxide and carbonate ions are major ligands present in most natural environments, so most important complexes of actinides contains these two anions (Runde 2000).

The only stable oxidation state of thorium is tetravalent, which is considered the least hydrolyzed of the known tetravalent metal ions due to its large ionic radius. Th(IV) is able to form monomeric species, (i.e., $Th(OH)^{3+}$, $Th(OH)_2^{2+}$, $Th(OH)_3^{1+}$, and $Th(OH)_4$)

and polymeric species (i.e., $Th_4(OH)_8^{8+}$ and $Th_6(OH)_{15}^{9+}$) (Ekberg et al. 2000; Rand et al. 2008). The hydrolysis reactions for thorium may be written as follows (Rand et al. 2008):

$$m\mathrm{Th}^{4+} + n\mathrm{H_2O}(l) \leftrightarrow \mathrm{TH_m(OH)}_n^{4m-n} + nH^+$$

Potentiometry, liquid-liquid extraction and solubility are the most frequently used approaches to determine the stoichiometry and equilibrium constants for the hydrolysis reactions (Rand et al. 2008). Various ionic media have been used to study the hydrolytic behavior of thorium over the years, including perchlorate (Baes et al. 1965; Ekberg et al. 2000; Grenthe 1991), nitrate (Brown et al. 1983; Milić and Šuranji 1982), and chloride (Milic 1981; Šuranji and Milić 1981). The Organization for Economic Co-operation and Development's (OECD) Nuclear Energy Agency (NEA) reviewed and organized previous relevant papers to publish a thorium thermodynamic reference book in 2008, and eventually selected the following most important hydrolytic reactions (Table 2.2) in pure water (Rand et al. 2008). Table 2.2 also shows the thorium hydroxide species and their constants with the most consistent results. Using the thermodynamic data in Table 2.2 and a Visual MINTEQ Model (Rand et al. 2008), a Th(IV) equilibrium speciation diagram was produced in a closed system with 0.001 M ionic strength background solution (Figure 2.1).

Table 2.2: Aqueous thorium hydrolysis reactions at T=25°C and I=0.0 M and associated Log K values. Log K constants were calculated from thermodynamic data given by Rand et al.(2008).

Species	Th(IV) Hydroxide Complexation Reactions	Log K
$Th(OH)^{3+}$	$Th^{4+} + H_2O(l) \leftrightarrow H^+ + Th(OH)^{3+}$	-2.500
$Th(OH)_2^{2+}$	$Th^{4+} + 2H_2O(l) \leftrightarrow 2H^+ + Th(OH)_2^{2+}$	-6.200
$Th(OH)_4(aq)$	$Th^{4+} + 4H_2O(l) \leftrightarrow 4H^+ + Th(OH)_4(aq)$	-17.400
$Th_2(OH)_2^{6+}$	$2Th^{4+} + 2H_2O(l) \leftrightarrow 2H^+ + Th_2(OH)_2^{6+}$	-5.900
$Th_2(OH)_3^{5+}$	$2Th^{4+} + 3H_2O(l) \leftrightarrow 3H^+ + Th_2(OH)_3^{5+}$	-6.800
$Th_4(OH)_8^{8+}$	$4Th^{4+} + 8H_2O(l) \leftrightarrow 8H^+ + Th_4(OH)_8^{8+}$	-20.400
$Th_4(OH)_{12}^{4+}$	$4Th^{4+} + 12H_2O(l) \leftrightarrow 12H^+ + Th_4(OH)_{12}^{4+}$	-26.600
$Th_6(OH)_{14}^{10+}$	$6Th^{4+} + 14H_2O(l) \leftrightarrow 14H^+ + Th_6(OH)_{14}^{10+}$	-36.800
$Th_6(OH)_{15}^{9+}$	$6Th^{4+} + 15H_2O(l) \leftrightarrow 15H^+ + Th_6(OH)_{15}^{9+}$	-36.800

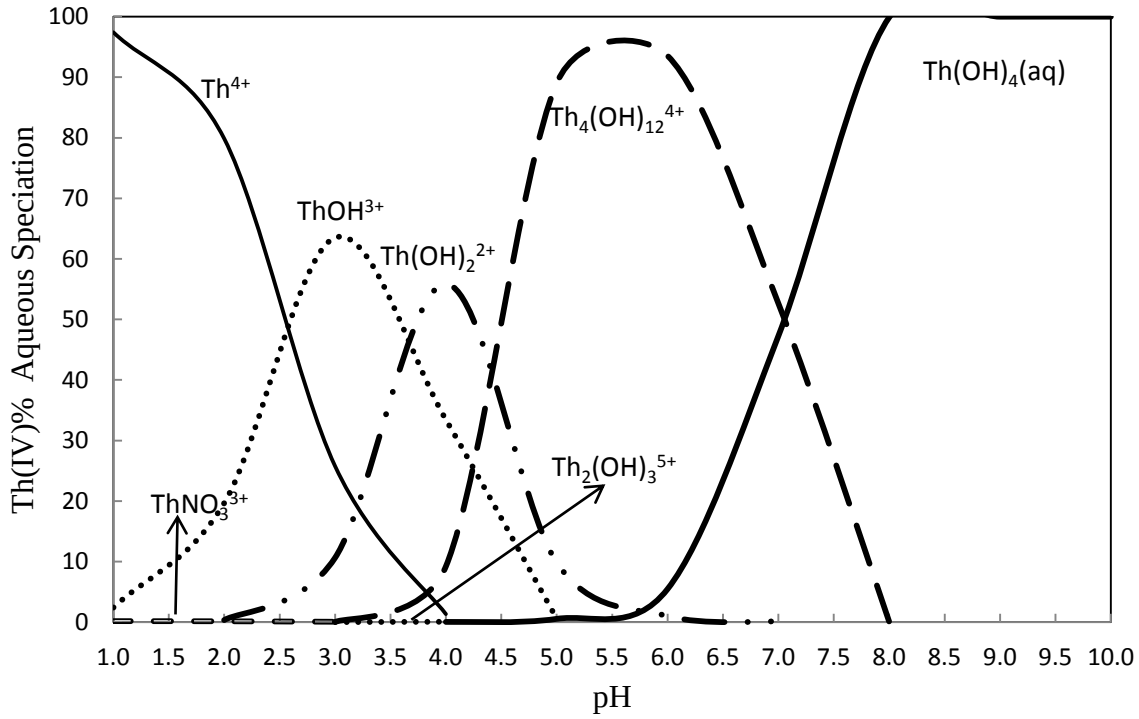

Figure 2.1: Aqueous distribution of 1.142×10^{-5} M Th(IV) as a function of pH calculated by Visual MINTEQ in a closed system with 0.001 M ionic strength.

Figure 2.1 shows that when thorium complexes with water with 0.001M ionic strength, there are seven distinct aqueous species present in the system, and five of them

will dominate in different ranges of pH. For example, the ionic form, Th^{4+} predominates in the acidic range (pH <2.6), while the aqueous form, $Th(OH)_4$ (aq) was the major thorium hydroxide in the basic pH range (pH >7). $Th(OH)^{3+}$, $Th(OH)_2^{2+}$ and $Th_4(OH)_{12}^{4+}$ predominate in the pH range from 2.6 to 3.7, 3.7 to 4.5, and 4.5 to 7, respectively.

In natural systems, carbonate is the other significant ligand existing in groundwater and also tending to complex with metal ions. The carbonate system is composed by various carbonate species involving gaseous carbon dioxide, CO_2(g), aqueous carbon dioxide, CO_2(aq), carbonic acid, H_2CO_3, bicarbonate, HCO_3^-, carbonate, CO_3^{2-}, and carbonate-containing solids (Snoeyink and Jenkins 1980). There were several studies with regard to thorium solubility and complexation in the carbonate system created in the laboratory by using CO_2(g) at different partial pressures ((Altmaier et al. 2006; Altmaier et al. 2005; Felmy et al. 1997; Östhols et al. 1994), or by using bicarbonate/carbonate (HCO_3^-/CO_3^{2-}) buffer solutions with a range of total carbonate concentration from 0.001 to 2.3 (Altmaier et al. 2006; Felmy et al. 1997; Melson 2012). The OECD NEA also reviewed and summarized this literature, and selected the most important thorium carbonate complxation reactions (Table 2.3). Using the thermodynamic data in Table 2.3 and Visual MINTEQ Model, a Th(IV) equilibrium speciation diagram was formed in an open system (log P_{CO2} =-3.5) with 0.001 M ionic strength background solution (Figure 2.2). Comparing with Figure 2.1 when hydroxide ion is the only ligand in the solution, there is no difference in species distribution at the pH range between 1 and 8, while above a pH of 8.5, thorium carbonate complexation predominates in the solution. Therefore, the introduction of carbonate will not influence the speciation of thorium at low pH ranges (pH<8).

Table 2.3: Aqueous thorium carbonate complexation reactions at T=25˚C and I=0.0 M and associated log K values. Log K constants were calculated from thermodynamic data given by Rand et al.(2008).

Species	Th(IV) Carbonate Complexation Reactions	Log K
$\mathbf{Th(CO_3)_5^{6-}}$	$\mathbf{Th^{4+} + 5CO_3^{2-} \leftrightarrow Th(CO_3)_5^{6-}}$	31.000
$\mathbf{ThOH(CO_3)_4^{5-}}$	$\mathbf{Th^{4+} + H_2O(l) + 4CO_3^{2-} \leftrightarrow H^{+} + ThOH(CO_3)_4^{5-}}$	21.600
$\mathbf{Th(OH)_2(CO_3)_2^{2-}}$	$\mathbf{Th^{4+} + 2H_2O(l) + 2CO_3^{2-} \leftrightarrow 2H^{+} + Th(OH)_2(CO_3)_2^{2-}}$	8.800
$\mathbf{Th(OH)_4(CO_3)^{2-}}$	$\mathbf{Th^{4+} + 4H_2O(l) + CO_3^{2-} \leftrightarrow 4H^{+} + Th(OH)_4(CO_3)^{2-}}$	-15.600

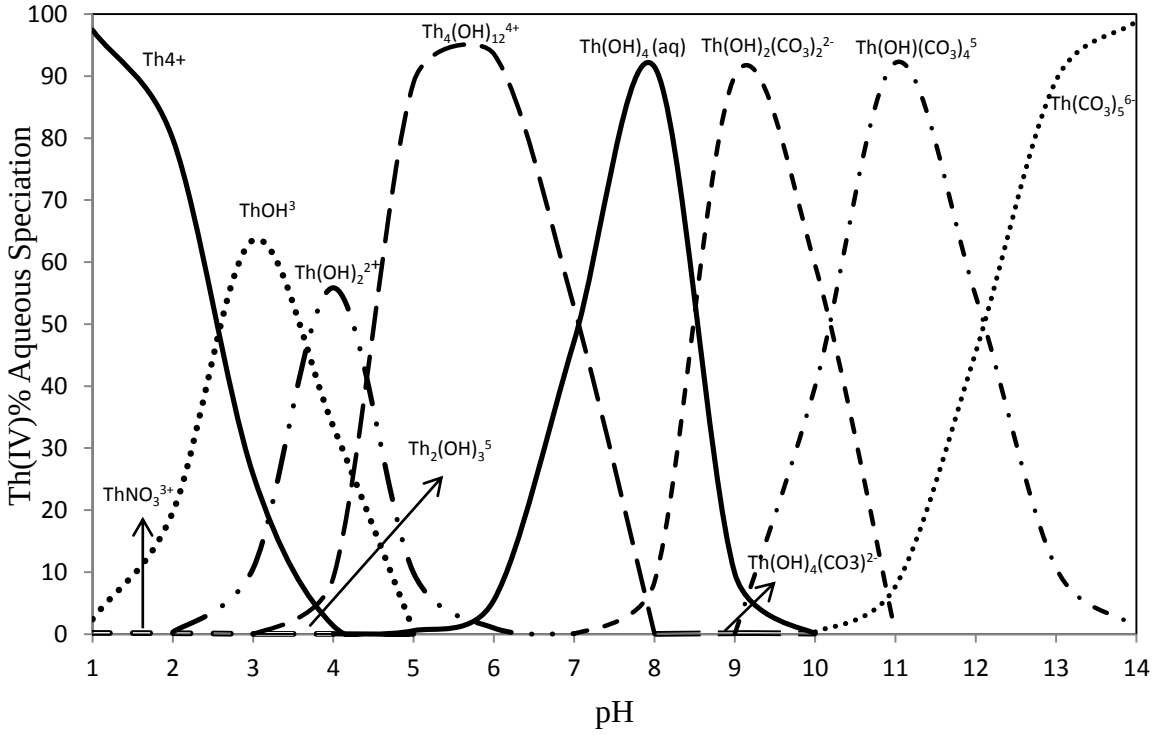

Figure 2.2: Aqueous distribution of 1.142×10^{-5} M Th(IV) as a function of pH calculated by Visual MINTEQ in a open system with Log P_{CO2}=-3.5 atm and 0.001 M ionic strength.

2.6 Thorium Solubility

Solubility, the amount of a solid in moles/liter or mg/liter dissolving in a solution under a given condition, is a very important property to study the fate and transport of contaminants (Snoeyink and Jenkins 1980). As an actinide concentration dissolves in

solution, solubility acts as the first barrier to its transport in the environment (Rand et al. 2008). Many factors can limit the solubility of a substance, like temperature, pressure, ionic strength, polarity and the size of solid (Snoeyink and Jenkins 1980). For actinides, the stability of the actinide-bearing solid and the stability of the complexed species in solution are the two primary properties affecting their solubility (Runde 2000). To understand the dissolution of a solid at equilibrium, it is necessary to introduce the concept of solubility product, Kso, an equilibrium constant that describes the reaction when a solid dissolves in pure water to form its ionic components, as seen below (Snoeyink and Jenkins 1980).

$$A_xB_y(s) \leftrightarrow xA^{y+} + yB^{x-}$$

The solubility product is then given by

$$K_{so} = \frac{\{A^{y+}\}^x\{B^{x-}\}^y}{\{A_xB_y(s)\}} = [A^{y+}]^x[B^{x-}]^y\{\gamma_{A^{y+}}\}^x\{\gamma_{B^{x-}}\}^y$$

where {i} indicates activity and [i] indicates concentration, and γ_i is the activity coefficient of species i. Therefore, the solubility of a substance can be calculated by a known K_{so} (Snoeyink and Jenkins 1980).

There have been considerable studies of the solubility of thorium oxides and hydroxides for many years. However, only two major experimental methods were used in most of thorium solubility research: solid-liquid equilibrium, which is adding an appropriate amount of the solid thorium oxides into a test solution and achieving equilibrium from the direction of undersaturation (Altmaier et al. 2004; Felmy et al. 1997; Kim et al. 2010; Östhols et al. 1994; Ryan and Rai 1987), and titration, which is titrating a constant concentration of acidic thorium solution until the formation of a solid precipitate or colloids is observed (Bundschuh et al. 2000; Neck et al. 2002). The first

method is conducted by measuring the concentration of thorium and pH as a function of time, while the titration method gives the pH value when the solubility is higher than the given total thorium concentration (Rand et al. 2008). The OECD NEA has reviewed and summarized these solubility studies, and eventually selected three reliable reactions of thorium solubility as shown in Table 2.4 (Rand et al. 2008). Using the thermodynamic solubility products in Table 2.4 and Visual MINTEQ Model, the log solubility of the three precipitates plot was formed as a function of pH (Figure 2.3).

Table 2.4: Th(IV) solubility reactions at T=25˚C and I=0.0 M and associated log K_{SO} values. Log K_{SO} constants were calculated from thermodynamic data given by Rand et al. (2008).

Precipitate	Th(IV) Solubility Reactions	Log K_{so}
ThO_2(am, hyd, fresh)	**$Th^{4+} + 2H_2O(l) \leftrightarrow 4H^+ + ThO_2$(am, hyd, fresh)**	-9.300
ThO_2(am,hyd, aged)	**$Th^{4+} + 2H_2O(l) \leftrightarrow 4H^+ + ThO_2$(am, hyd, aged)**	-8.500
ThO_2(cr)	**$Th^{4+} + 2H_2O(l) \leftrightarrow 4H^+ + ThO_2$(cr)**	-1.766

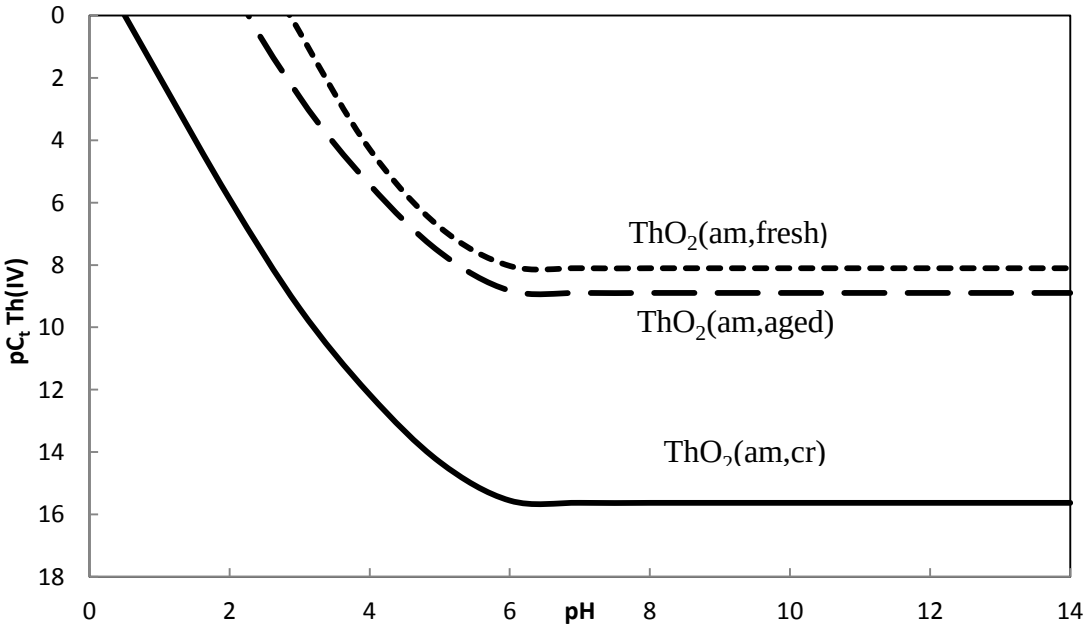

Figure 2.3: Solubility of Th(IV) precipitates as a function of pH, calculated by Visual MINTEQ in a closed system with 0.001 M ionic strength.

The hydrated oxyhydroxide $ThO_n(OH)_{4-2n}\ xH_2O(am)$ with $0<n<2$ instead of $ThO_2(s)$ is the primary component of the amorphous Th(IV) precipitates ($Th(OH)_4(am)$ or ThO2(am, hyd)), which are not well-defined compounds (Rand et al. 2008). Unlike amorphous solids, the crystalline thorium precipitates have a highly organized structure (Haliena 2012; Rai et al. 2000). As seen from Table 2.4 and Figure 2.3, the solubility of the amorphous and crystalline thorium precipitates varies about 8 orders of magnitude but is independent of pH when the solution approaches to neutral and basic conditions. The primary reason for the discrepancies of thorium solubility in the two different forms is particle size and surface hydration (Rand et al. 2008). Due to the lengthy process of the transformation from amorphous thorium hydroxides to crystalline thorium dioxide (about 270 days), the solubility of thorium in natural systems is controlled by amorphous thorium hydroxides (Haliena 2012; Prasad et al. 1967; Rai et al. 2000; Rand et al. 2008).

2.7. Th(IV) Sorption onto Metal Oxides and Clay Minerals

The sorption of thorium onto the surface of soil grains is considered to be the second primary barrier to its migration or transport in the groundwater (Rand et al. 2008). There are many factors impacting the process of actinide sorption onto mineral surfaces, such as the concentration and speciation of actinides, the groundwater flow rate and its chemistry, and the composition of the surrounding minerals. Moreover, different physiochemical mechanisms can cause actinides to attach to a mineral/rock surface to prevent its transport, including physical adsorption, ion exchange, chemisorption, and surface precipitation (Runde 2000). Therefore, understanding actinides' sorption characteristics can help to predict their migration through the environment.

Metal oxides and clay minerals are two major absorbents frequently used to study Th(IV) adsorption. In the experiments of Th(IV) sorption onto the various metal oxides including magnetite (Rojo et al. 2009; Seco et al. 2009), goethite ((Hunter et al. 1988; Reiller et al. 2002), hematite (Cromieres et al. 1998; Murphy et al. 1999), silica (Chen and Wang 2007; Li and Tao 2002; Östholsetal. 1997), aluminum oxides (Guo et al. 2005; Hongxia et al. 2006), titania (Anna-Maria 1999; Tan et al. 2007; Zhijun et al. 2005), and manganese oxides (Hunter et al. 1988), most of the results showed that Th(IV) sorption was pH dependent but independent of ionic strength. However, two papers demonstrated that greater ionic strength could cause the lower adsorption of thorium (Guo et al. 2005; Zhijun et al. 2005). Therefore, Zhijun et al (2005) concluded that the concentration of the metal, the ionic strength range, and the cation and anion background solution, all can affect the sorption of a metal onto an oxide.

In the experiments of Th(IV) sorption onto the different types of common clays including kaolinite (Banik et al. 2007), bentonite (Zhao et al. 2008), and montmorillonite (Chen et al. 2006; Pshinko et al. 2009), results showed that Th(IV) is strongly adsorbed to various clays over the pH range of 1 to 3, indicating that surface complexation reactions dominate the sorption mechanism. Moreover, these studies also revealed that Th(IV) has a stronger affinity for clay mineral than metal oxides. Therefore, Th(IV) transport in the groundwater is possibly retarded due to adsorption, since most soils and rocks consist of metal oxides and clay minerals.

2.8 Colloid-Associated Contaminant Transport

It was believed for more than two decades that the transport of contaminants in groundwater aquifers was related only to two phases (the soil liquid phase and gaseous

phase), and their distribution in the saturated subsurface zone depended on the immobile solid phase and the mobile aqueous phase. When this two-phase equilibrium adsorption system was used to predict the fate of contaminants, many metals and radionuclides with a strongly affinity to soil grains were expected to be fixed in the subsurface, presenting little threat to groundwater supplies. However, low-solubility contaminants were discovered far away from a known source, which led to the examination of the possible existence of mobile colloids and the development of a three-phase model involving a mobile liquid phase, a mobile colloidal phase, and the immobile solid phase in contaminant transport (as shown in Figure 2.4) because the inclusion of colloidal particles can well explain such phenomenon (Honeyman 1999; Kersting et al. 1999; Sen and Khilar 2006; Sen et al. 2002). Therefore, the theory that the soil solid phase in addition to the mobile soil particles and colloids is capable of impacting the migration of contaminants as well is now generally accepted by many researchers (Elimelech and Ryan 2002; Honeyman 1999; Kersting et al. 1999; Saiers and Lenhart 2003; Sen et al. 2002). Current colloid-associated contaminant transport models hold that colloidal fines present in groundwater can facilitate as well as retard the transport of contaminant (Kanti Sen and Khilar 2006; Sen and Khilar 2006).

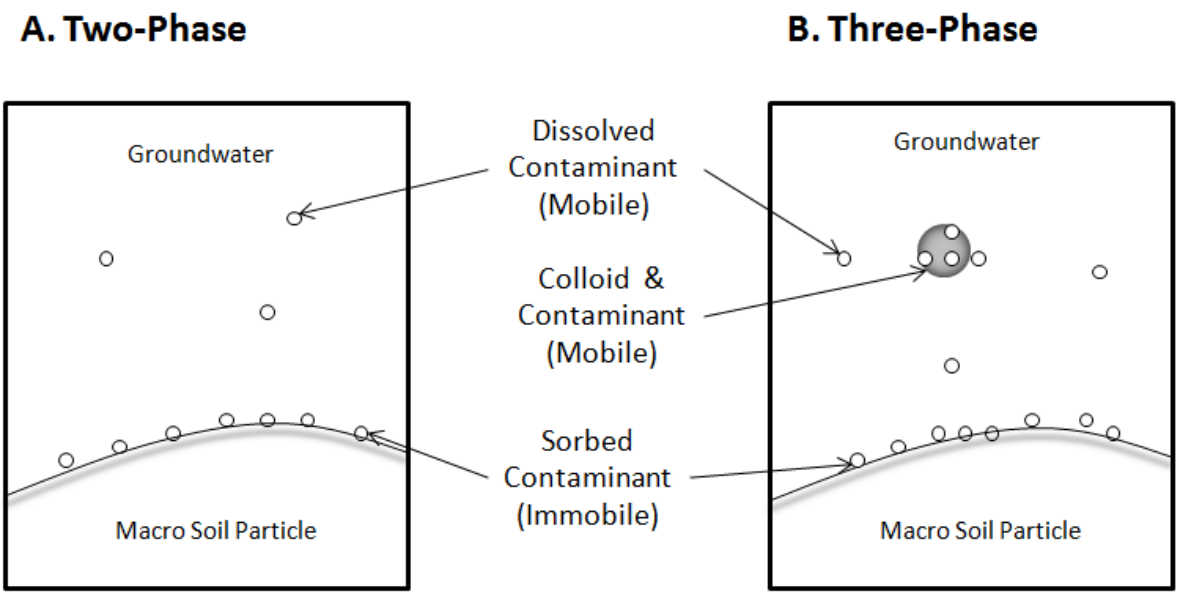

Figure 2.4: Comparison of two (A) and three (B)-phase contaminant transport models in groundwater system. Adapted from McCarthy et al. (1989).

2.8.1 Source of Colloid and Its Release Mechanisms in the Groundwater

Colloidal fines, ubiquitous in the natural aqueous environments, consist of a variety of inorganic and organic materials including rock fragments, clay minerals (e.g. kaolinite, illite), mineral precipitates (e.g. Fe, Al, Mn, or Si oxides and hydroxides, carbonates, phosphates), organic biopolymers (e.g. humic and fulvic acids), and biocolloids (e.g. bacteria and viruses) (Kanti Sen and Khilar 2006; Kretzschmar and Schafer 2005; McCarthy and Zachara 1989; Sen and Khilar 2006). They are classified as migratory particles with dimensions between 1 nm to 10 μm with a high specific surface area (10-800 m^2g^{-1}) (Figure 2.5) and generally carry electric charge on their surface (Figure 2.6) (Kersting et al. 1999; McCarthy and Zachara 1989). There are several potential sources generating colloidal particles in groundwater systems including *in situ* mobilization of naturally existing fine minerals, precipitation of supersaturated mineral

phases, and direct introduction through man-made waste management procedures like landfills (McCarthy and Zachara 1989; Ryan and Elimelech 1996; Sen and Khilar 2006).

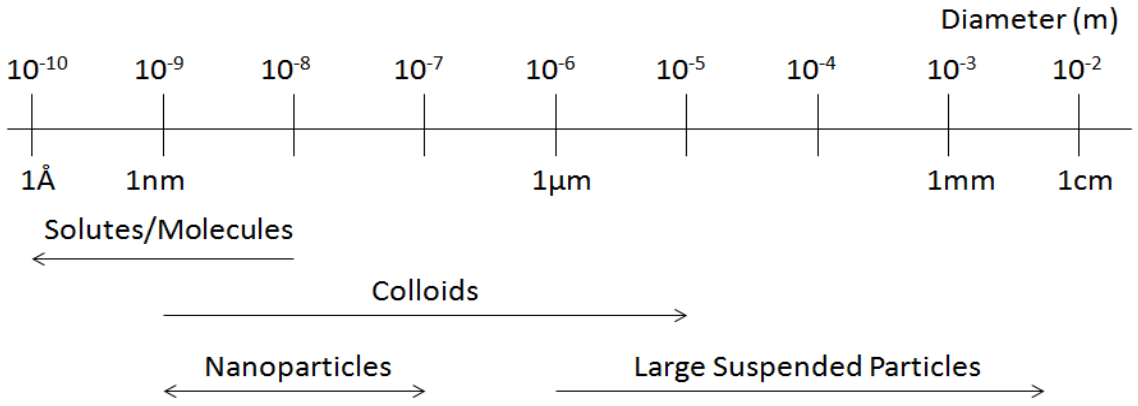

Figure 2.5: Size spectrum of waterborne particles. Adapted from McCarthy et al. (1989).

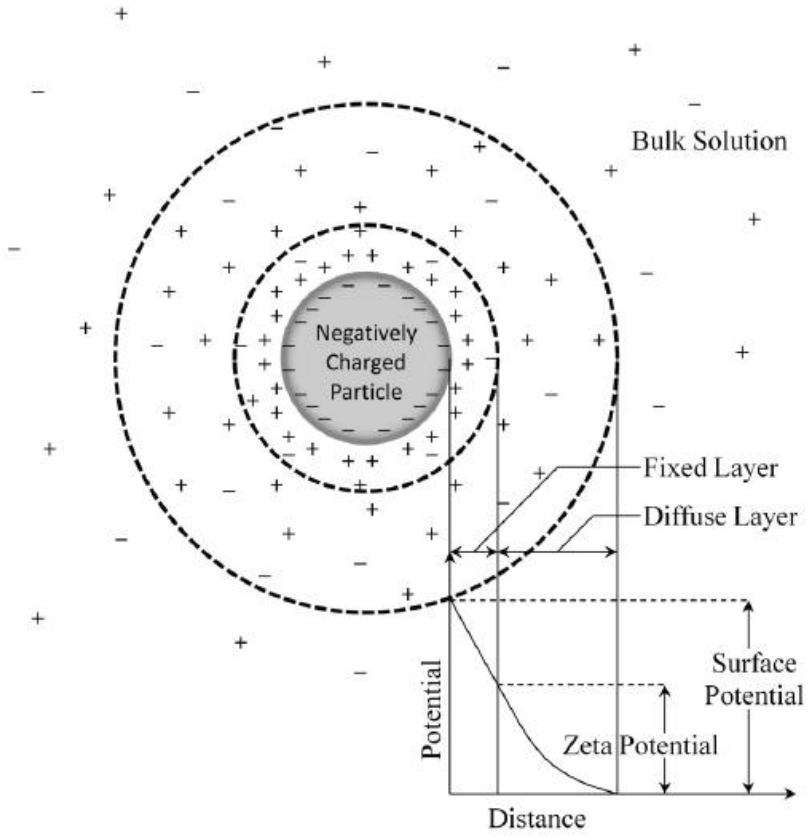

Figure 2.6: Electrostatic field of a negatively charged colloidal particle. Adapted from Priesing (1962).

Due to the various sizes of colloids, the interactions among colloidal fines are different. When colloidal particles are bigger than 1 μm, the major interaction among them are physical forces like gravity or fluid drag, while interfacial characteristics of the particle solution will control the interactions among submicron particles (1 nm-1 μm) (Bin et al. 2011; Bin 2011; Stumm 1977). Most colloids contained in groundwater sediments are immobile under stable physical and chemical conditions, but can be released from the soil matrix by fluctuations in flow velocity, water saturation, and solution chemistry (Kretzschmar and Schafer 2005; McCarthy and Zachara 1989; Ryan and Elimelech 1996). Although high flow rates causing colloid release from soil owing to the hydraulic shear stress on particles has been demonstrated in many laboratories, it should not be the primary reason in nature because the groundwater is known for a low flow rate, typically around 0.00002 km/hr (Kaplan et al. 1993; Nelson 2012; Sharma et al. 1992).

The most common source of mobile colloids in the subsurface derives from changes in solution chemistry, such as decreases in ionic strength, or increases in pH, variations in redox potentials, and adsorption of solutes that alter mineral surface charges. (Grolimund 1999; McCarthy and Zachara 1989; Ryan and Elimelech 1996). For example, Haliena (2012) found in the column transport experiment in the absence of Th(IV) that an increase in solution pH from 4 to 11 promoted the mobilization of natural colloids including goethite and kaolinite from the surface of Savannah River Site (SRS) sediment (Figure 2.7). The mechanism of this chemically induced release is that when the net effect of electrical double layer repulsion and London-Van der Waals attraction between the colloidal fines and the matrix surface is negative, the fine particle may be released

(Kanti Sen and Khilar 2006; Ryan and Elimelech 1996; Sen and Khilar 2006). The net effect of these attractive and repulsive forces is also called the DLVO (Derjaguin, Landau, Verwey and Overbeek) theory, which describes the potential energy profile for colloidal fine and grain surface interactions by summing the double layer, London-Van der Waals and short-range repulsive forces over the interaction distance between them (Figure 2.8). Once the colloids are released from the soil grain surface, they can either re-adhere to the surface when the condition changes again, flow without capture, or get entrapped at the pore constrictions while flowing with the fluid through the porous media (Sen and Khilar 2006).

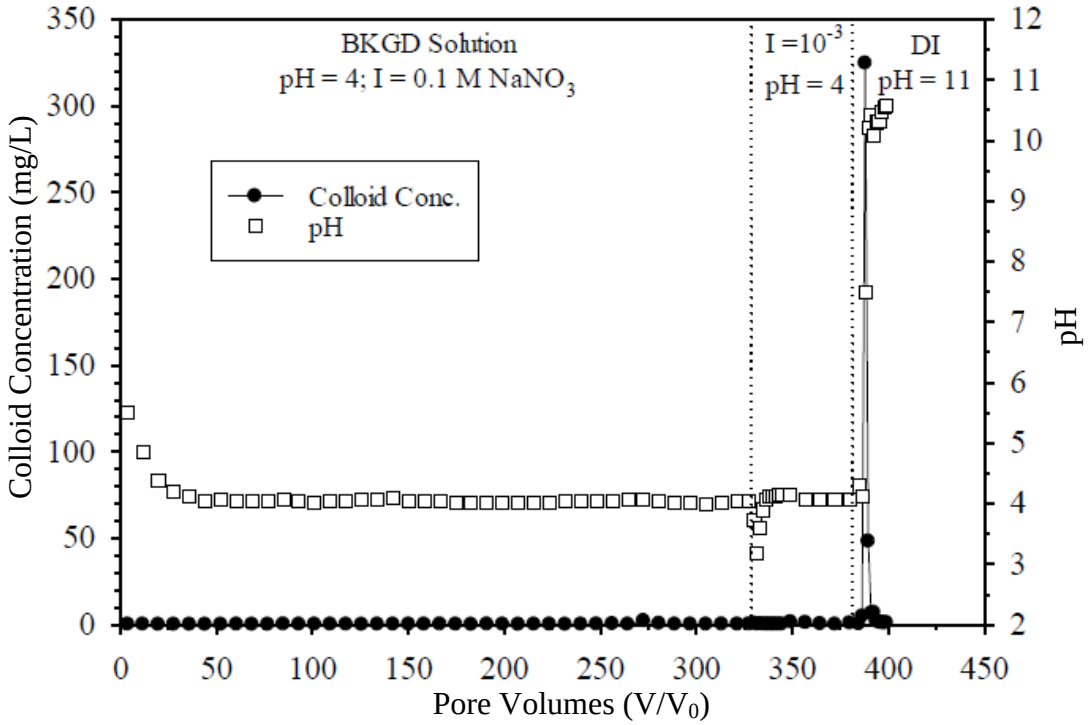

Figure 2.7: Effluent colloid concentration and pH from Savannah River Site (SRS) sediment in Th(IV)-free transport experiment (Temp=26±1°C, Q=6 mL/hr). Cited from Haliena (2012).

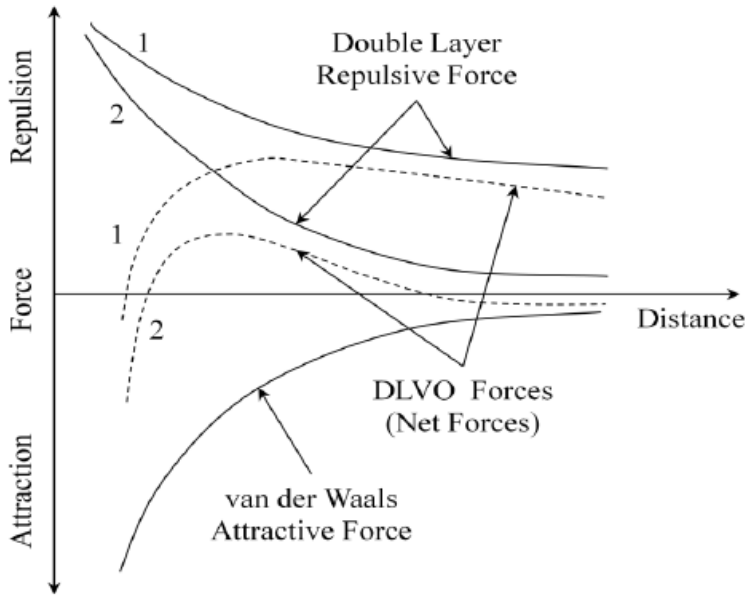

Figure 2.8: Interparticle forces vs. distance at low electrolyte concentrations (1) and high electrolyte concentrations (2). Cited from Pitts (1995).

2.8.2 Colloid-Facilitated Transport of Contaminant

When migrating in subsurface, colloidal fines would minimally interact with the soil matrix on which some low-solubility chemicals or contaminants are attached. The solubility of contaminants would be increased during the course of interaction between colloids and minerals. Meanwhile those contaminants having a strongly affinity to the colloids can transport with those fine particles. This contaminant transport has been known as colloid-facilitated contaminant transport (Kanti Sen and Khilar 2006; Sen and Khilar 2006). Numerous studies have shown that colloid-facilitated transport may be one of the most significant mechanisms for the movement of contaminant species in soils (Barton and Karathanasis 2003; Grolimund 2005; Kretzschmar and Schafer 2005). Bergendahl and Grasso (2003) developed a particle release model under various geochemical conditions to predict the behavior of *in situ* colloids following a change in

ionic strength. Their results suggested that if the disturbance of ionic strength took place in the porous media in the presence of sorbing contaminants, the mobilized particles maybe possibly act as carrier for facilitating contaminant transport (Bergendahl and Grasso 2003). Another conceptual model that included transported colloidal particles in radionuclide migration showed that the retardation factor for strongly retained ions like Am and Th could be reduced by several orders of magnitude because of colloidal transport (Contardi et al. 2001). In addition, laboratory experiments conducted by Saiers and Hornberger (1999) also implied that under the condition of low ionic strength, colloidal kaolinite is capable of accelerating ^{137}Cs migration in saturated porous media.

2.8.3 Colloid-Retardant Transport of Contaminant

As mentioned earlier, the released colloidal fine can either re-adhere to the soil surface once the condition changes again, flow without capture, or get entrapped at the pore constrictions while flowing with the fluid through the porous media (Sen and Khilar 2006). However, the possibility of colloidal particles flowing free and being blocked is much higher than that of re-adhering back to soil because conditions in groundwater are rather stable (Sen and Khilar 2006). There are three ways that colloids can be entrapped at the pore constriction including size exclusion, multi-particle bridging, and surface deposition (Khilar and Fogler 1998). Furthermore, Zhu et al (2012) demonstrated that mercury (Hg) mobility was reduced by the presence of kaolinite in sand column due to the increasing deposition rate of Hg-loaded kaolinite. Therefore, it is necessary to study colloid-retardant transport in order to help predict the migration of contaminants and develop a new technique for immobilization of contaminants in groundwater.

Chapter Three

The Influence of Colloidal Kaolinite on Th(IV) Transport in Saturated Porous Media

This Chapter serves a draft manuscript manuscript. It will later be submitted for publication to a peer-reviewed scientific journal.

3.1 Introduction

Radioactive waste has been an important environmental concern since the 1940s, because substantial amounts of radioactive materials have been used in nuclear weapon programs and nuclear power industries and many of them have accumulated as waste (Ahearne 1997). Due to improper nuclear handling and storage, a large amount of actinides have spilled into groundwater, contaminating the aquifer system and potentially jeopardizing human health (Ahearne 1997; Runde 2000). Actinides, which have electrons that fill the 5f orbitals, exhibit multiple oxidation states and are capable of forming numerous molecular species (Runde 2000). In these distinct valences of actinides, tetravalent ions (An (IV)) readily hydrolyze to form the strongest and most stable complexes in water, while the ability of pentavalent actinide ions (An (V)) to form complexes is the weakest. In other words, An (IV) species have a strong tendency to adsorb onto rock or mineral surfaces and have low solubility in the groundwater (Neck and Kim 2001; Runde 2000). Therefore, actinides were initially expected to be immobile in porous media because of their low concentration and strong affinity for the solid phase

(Kersting et al. 1999). However, subsequent field reports showed that actinides were detected long distances from the waste sites (e.g., five out seven waste sites detected trace plutonium(Pu) away from the source, and the longest migration distance is 4 km at Mayak Production Association in Russia) (Cantrell and Riley 2008; Kaplan et al. 1994; Penrose et al. 1990). Many studies have demonstrated that colloids, classified as migratory particles with dimensions between 1 nm to 10 μm and a high specific surface area (10-800 m^2g^{-1}), were responsible for these unanticipated migrations of transition metals and actinides in soils and aquifers (Ryan and Elimelech 1996). Under some specific conditions, significant quantities of colloids can be released from the solid aquifer matrix by chemical perturbations like a decrease in ionic strength, increases in pH or adsorption of solutes that alter mineral surface charges (Burgisser et al. 1993; Grolimund 2005; McCarthy and Zachara 1989; Neretnieks and Rasmuson 1984; Sardin et al. 1991). Once colloids are free, they migrate by advection and dispersion or redeposit due to mass transfer reactions that happen at mineral-grain surfaces and the air-water interface (Saiers and Lenhart 2003; Sen and Khilar 2006). Most importantly, the contaminants strongly adsorbed on colloidal particles would flow along with colloids into the groundwater aquifers and potentially affect the quality of drinking water (McGechan and Lewis 2002; Ryan et al. 1998; Sprague et al. 2000).

At many Department of Energy sites, Pu has been detected migrated away from the sources (Cantrell and Riley 2008). For examples, trace Pu was detected in groundwater 1.3 km from Nevada Test site. However, it is extremely difficult to study Pu in the laboratory because its III, IV, and V oxidation states can co-exist in the normal range of natural waters (Choppin 2007; Runde 2000). Fortunately, Pu(IV) is the most

prevalent oxidation state in most subsurface environments, and actinides in the same oxidation state tend to behave similarly (Choppin 1999; Guo et al. 2005; Hongxia et al. 2007; Hongxia et al. 2006). Consequently, thorium (Th(IV)) which exists only in one oxidation state in the environment may be used as an analog for Pu(IV) to study whether inorganic colloid transport is the key to facilitate the migration of tetravalent actinides (Choppin 2007). There is a significant body of literature on the colloid-facilitated transport of contaminants, but limited research examined colloid-associated transport of actinides including both facilitation and retardation influence. Hence, the objectives of this study were (1) to determine the transport of colloidal kaolinite and Th(IV) in saturated porous media, (2) to investigate colloid-facilitated transport and its effect on Th(IV) migration by comparing the transport behavior of colloidal Th(IV) (Th(IV) adsorbed onto kaolinite before transport) and soluble Th(IV), (3) to test whether kaolinite can scavenge Th(IV) adsorbed onto sand media, and (4) to examine the possibility of colloid-associated retardation of contaminants by comparing Th(IV) transport in sand columns with and without kaolinite present.

3.2. Materials and Methods

3.2.1 Chemical Solutions

All chemicals employed in this study were ACS grade and purchased from VWR International LLC or Fisher Scientific. The Th(IV) stock solution was prepared by dissolving solid $Th(NO_3)_4$ $4H_2O$(s), obtained from International Bio-Analytical Industries Inc., in 0.07 M HNO_3. The ionic strength of the background electrolyte was adjusted with $NaNO_3$, and the pH of solution was adjusted by using 0.1 M HNO_3 and 0.0715 M NaOH.

Aqueous Th(IV) standards were diluted from a thorium atomic absorption standard from Sigma-Aldrich with a 0.1 M HNO_3 solution at a 0.001 M ionic strength, similar to all other solutions and samples.

3.2.2 Colloidal Suspension and Porous Medium

The kaolinite stock suspension was prepared by adding 0.8 g of kaolinite powder (EMD Chemicals, Inc.) in 1000 ml of deionized water (18.2 MΩ cm), then shaking vigorously before placing in an ultrasonic dispersion bath for 30 min and pipetting approximately 300 ml of suspension to an empty bottle after 24 hours. The mass of kaolinite solution was determined gravimetrically, and the concentration of colloidal particles ranging from 291 mg/L to 299 mg/L (average 295±4 mg/L) was measured by turbidity with a Hach 2100N Laboratory Turbidmeter. The suspension of kaolinite was prepared by diluting the stock solution above and adding 0.001 M $NaNO_3$ and 1.037×10^{-4} M HNO_3. Sediments used as the porous medium in the column experiments were mineralogically pure and heat-resistant quartz sands, obtained from Unimin Corporation.

3.2.3 Column Transport Experiments

Transport experiments were conducted in 2.5 cm diameter Omnifit Labware (Diba) glass columns. Each column was wet-packed with an average mass of 93.4 g of pure quartz sand to an average height of 12.10 cm of 2.5 cm inner diameter (ID), which corresponds to an average bulk density of the pure quartz of 1.574±0.004 g/cm^3. Therefore, assuming an average particle density of 2.65 g/cm^3 for well-defined quartz, the average porosity was 0.406±0.002 which gives an average pore volume of 24.085±0.030 mL. The columns were oriented vertically and sealed at the top and bottom

with adjustable and fixed end piece fittings, respectively. Moreover, 50-μm PTFE frits were used at each end piece, which retained the pure quartz sands but allowed the solution and mobile colloids to pass through the column. To prevent colloidal kaolinite in the inlet solution from settling, a stirrer was used during the course of experiment.

Two HPLC pumps with a valve switch were used in the column system to allow for step feeds. Prior to the start of the experiment, a background solution with 0.001 M $NaNO_3$ at a pH of 4.0 was running through the sand-packed column upward for 48 hours at a constant specific discharge of 0.2 cm/min to fully saturate and stabilize the pH of the system. Low ionic strength was used to decrease the possibility of coagulation of colloidal suspension (Ryan and Elimelech 1996). The pH in groundwater depends on the composition of sediments and rocks, but using a pH of 4.0 in this study was mainly determined by the solubility of ThO_2, shown in Figure 3.1. The suggested equilibration times to distinguish between ThO_2(am, fresh) and ThO_2(am, aged) are <25 days and >70 days, respectively (Rand et al. 2008). However, Melson (2012) demonstrated that even in short-term experiments the solubility of Th(IV) in solutions is apparently controlled by ThO_2(am, aged), not ThO_2(am, fresh) for 3.3×10^{-5} M Th(IV) in 0.09 M $NaNO_3$ and 0.01 M $NaHCO_3$ (Figure 3.2). Moreover, Melson (2012) concluded that Th(IV) sorption onto colloidal kaolinite was strong from pH 2 to 5. Bromide, as a conservative tracer, was applied to determine the column hydrodynamic property, which yielded an average dispersion coefficient of 0.038 ± 0.016 cm^2/min (column Peclet Number ranges from 107.58 to 224.59) (Table A.1).

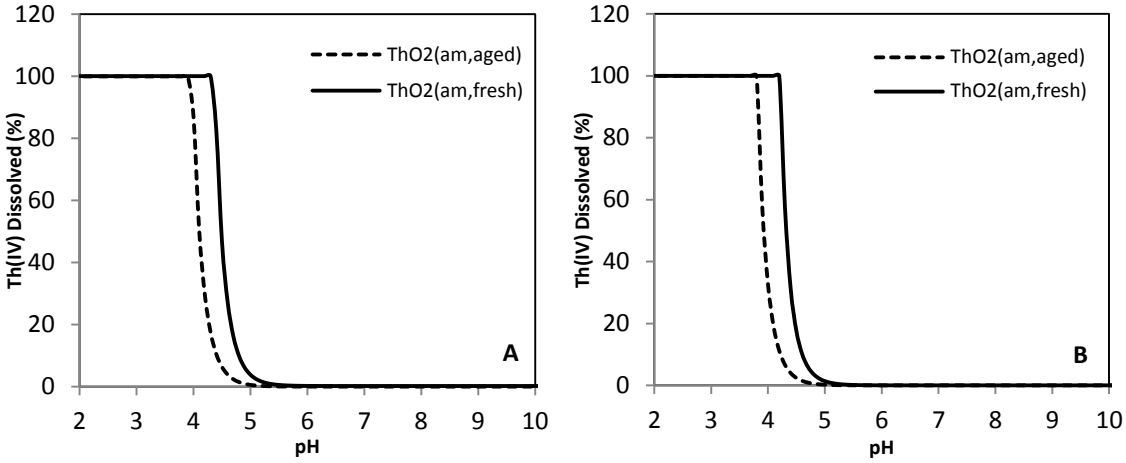

Figure 3.1: Theoretical dissolved percent for different concentrations of Th(IV) at 0.001 M ionic strength as a function of pH (C_{Th} = 1 mg/L = 4.31 × 10^{-6} M in plot A, C_{Th} = 2.65 mg/L = 1.14 × 10^{-5} M in plot B), calculated by Visual MINTEQ based on solubility of ThO_2(am, fresh) (solid line) and ThO_2(am, aged) (dashed line).

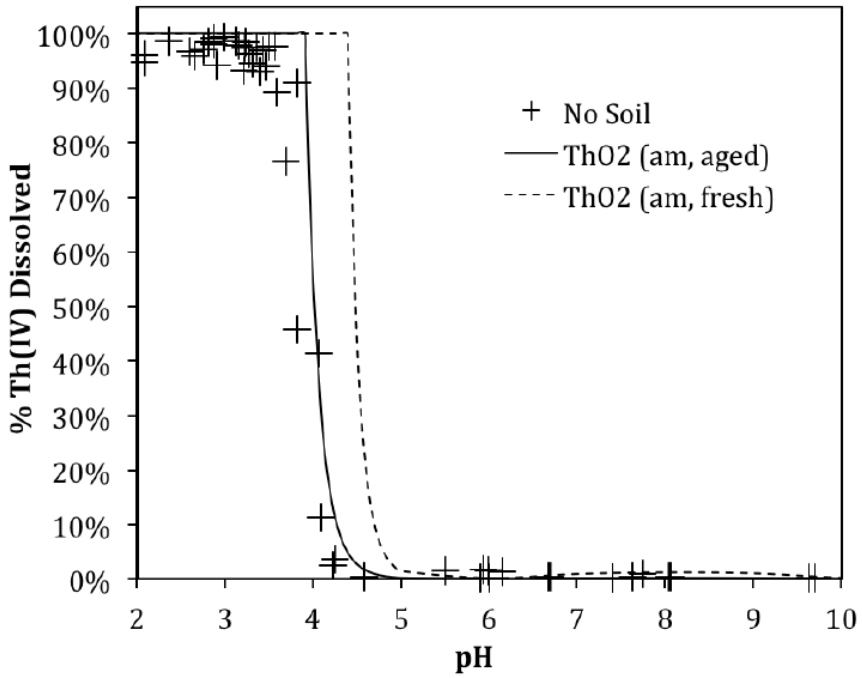

Figure 3.2: Measured Th(IV) removal percent for samples containing no soil (+) compared to theoretical curves based on the solubility of ThO_2(am, fresh) (dashed line) and ThO_2(am, aged) (solid line) as a fuction of pH (C_{TTh} = 3.3 × 10^{-5} M, 0.09 M $NaNO_3$, 0.01 M $NaHCO_3$, T=25°C). Copied from Melson (2012).

There were three types of column experiments: transport, colloid-facilitated transport, and colloid-retardant transport. All column experiments were divided into three

phases including a saturation phase, sorption phase and desorption phase. The sorption phase was initiated after the column was saturated with background solution, allowing target solution to adsorb to the pure quartz sands, and background solution was introduced into the column again to encourage the substance to desorb from the grains. The saturation phase and desorption phase used identical background solutions in the same experiment, while the influent solutions in the sorption phase vary with different experiments including 100 mg/L kaolinite, 1 mg/L ($4.31x10^{-6}$ M) Th(IV), 2.65 mg/L ($1.14x10^{-5}$ M) Th(IV), and 100 mg/L kaolinite suspension with different concentration of Th(IV). Samples of effluent were collected with a fraction collector at fixed time intervals. All transport experiments were conducted in duplicate, and all solutions involved in experiments are at a pH of 4.0 and 0.001 M ionic strength. The conditions for different column experiments are shown in Table 3.1.

Table 3.1: Column transport experiments conditions

Description	Column ID	Composition of Influent solution		
		Saturation Period (Phase I)	**Sorption Period (Phase II)**	**Desorption Period (Phase III)**
Transport	Exp #1	0.001M $NaNO_3$, pH 4.0	100 mg/L kaolinite, I=0.001M, pH 4.0	0.001M $NaNO_3$, pH 4.0
	Exp #2	0.001M $NaNO_3$, pH 4.0	1 mg/L Th(IV), I=0.001M, pH 4.0	0.001M $NaNO_3$, pH 4.0
	Exp #3	0.001M $NaNO_3$, pH 4.0	2.65 mg/L Th(IV), I=0.001M, pH 4.0	0.001M $NaNO_3$, pH 4.0
Colloid-Facilitated Transport	Exp #4	0.001M NaNO3, pH 4.0	100mg/L kaolinite & 1mg/L Th(IV) mixture, I=0.001M, pH 4.0	0.001M NaNO3, pH 4.0
	Exp #5	0.001M NaNO3, pH 4.0	100mg/L kaolinite & 2.65 mg/L Th(IV) mixture, I=0.001M, pH 4.0	0.001M NaNO3, pH 4.0
Colloid-Retardant Transport	Exp #6	100mg/L kaolinite, I=0.001M, pH 4.0	1mg/L Th(IV), I=0.001M, pH 4.0	100mg/L kaolinite, I=0.001M, pH 4.0
	Exp #7	100mg/L kaolinite, I=0.001M, pH 4.0	2.65mg/L Th(IV), I=0.001M, pH 4.0	100mg/L kaolinite, I=0.001M, pH 4.0
	Exp #8	1mg/L Th(IV), I=0.001M, pH 4.0	100mg/L kaolinite, I=0.001M, pH 4.0	1mg/L Th(IV), I=0.001M, pH 4.0
	Exp #9	2.65mg/L Th(IV), I=0.001M, pH 4.0	100mg/L kaolinite, I=0.001M, pH 4.0	2.65mg/L Th(IV), I=0.001M, pH 4.0

3.2.4 pH, Turbidity, and Th(IV) Concentration

After collecting all effluent samples, the pH was measured with a pH meter and combination electrode (Thermo Orion Model 410 A+) calibrated with standard buffer solutions. For effluents containing kaolinite, the concentration of colloids was correlated to turbidity which was analyzed with a Hach 2100N Laboratory Turbidimeter. To minimize precipitation, kaolinite samples were shook for 20 s by a Vortex mixer and then let stand for 10 s before putting in Turbidimeter. For samples containing both Th(IV) and kaolinite, an aliquot was removed to measure pH and turbidity, and the remainder was analyzed Th(IV) concentration by a Varian 710-ES ICP-OES at a low pH. To make effluent samples acidified, 5% by volume of 2 M HNO_3 were added giving solutions a pH of 1.0 to ensure Th(IV) totally dissolved and to prevent Th(IV) being adsorbed to sample tube walls. In addition, Teflon tubes were used in all experiments to collect effluent for minimization Th(IV) loss by absorption to tube walls (Haliena,2012).

3.2.5 Jar testing

Jar testing is a pilot-scale test used in water treatment plants to help operators determine the optimum coagulant dose for turbidity removal (Satterfield 2005). However, in this study it was used to examine the potential destabilization effects of Th(IV) on colloidal kaolinite suspensions. When the amount of Th(IV) is great enough to destabilize colloidal kaolinite, they will occur coagulation and flocculation, resulting in precipitation finally. However, if the amount of Th(IV) is insufficient, they might form pseudo-colloids that Th(IV) is totally adsorbed onto surfaces of kaolinite (Jeong et al. 2011). The pseudo-colloids have been assumed to mobilize in the aqueous system, which enhance the migration of insoluble contaminations through the subsurface (Haliena 2012; Kim

1991; Melson 2012). The procedure of the Jar Test is as follows: (1) prepare six beakers containing 100 mg/L kaolinite and different concentration of Th(IV) ranging from 0 to 3.5 mg/L with 0.001 M ionic strength at a pH of 4.0, (2) mix for 30 seconds at high speed (183 rpm) and then for 30 minutes at 40 rpm with a jar test apparatus, (3) finally allow to stand for 30 minutes to allow settling.

3.3 Results and Discussion

3.3.1 Jar test

The dosage of coagulants reach at a certain amount capable of destabilizing colloids and binding them into large and heavier flocs which precipitate relatively fast, but it is unknown about the conditions between colloids and coagulants existing in one solution when colloids are underfeeding. As seen from Figure 3.3, Th(IV) as a coagulant could remove turbidity caused by kaolinite. When 2 mg/L Th(IV) was added into 100 mg/L kaolinite solution, approximately 80% of both kaolinite and Th(IV) were removed from solution. As the Th(IV) concentration reached 3.5 mg/L, kaolinite and Th(IV) both were reduced to 10% of the initial concentration. However, neither Th(IV) nor kaolinite were removed in samples containing equal or less than 1 mg/L of Th(IV). No dissolved Th(IV) concentration, determined after filtration with 0.45 μm membrane filters, was detected in samples of 0.5 mg/L and 1.0 mg/L, and suspensions of 2 mg/L and 3.5 mg/L. Haliena (2012) demonstrated that 0.2 μm membrane filters allowed 2.64 mg/L dissolved Th(IV) to totally pass through. Therefore, low concentration of Th(IV) ($\leq$ 1 mg/L) could produce mobile pseudo-colloids with 100 mg/L kaolinite, potentially indicating high possibility of colloid-facilitated transport of Th(IV).

However, ≥ 2mg/L Th(IV) coagulating with 100 mg/L kaolinite caused significant aggregation, and at least 80% turbidity removal. There are two possible situations for high concentration of Th(IV) binding with colloids. One is Th(IV) ions

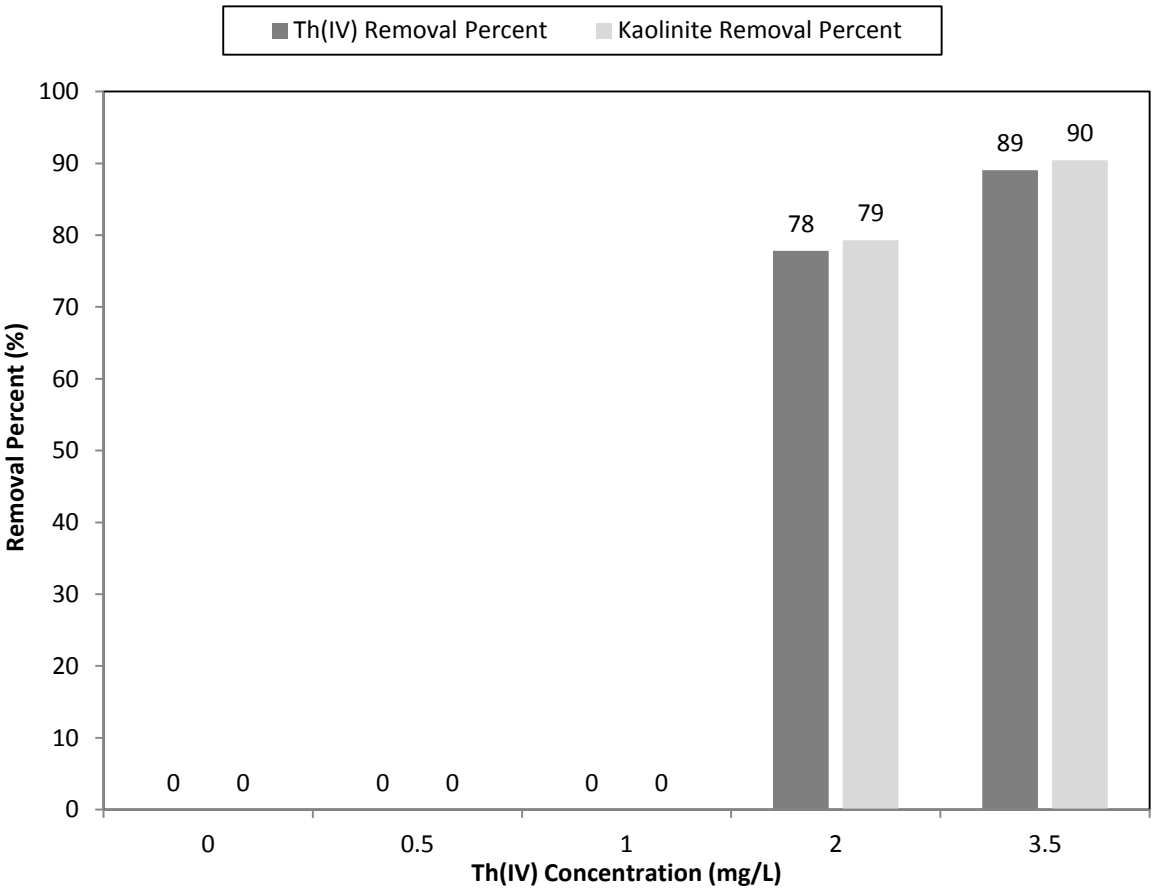

Figure 3.3: Percent removal of Th(IV) and colloidal kaolinite solution in Jar Test: dark color of columns indicates the concentration changes of Th(IV), and light color of columns indicates the concentration changes of kaolinite.

complex with kaolinite to make them both settle due to charge neutralization. The other is that high level of Th(IV) forming to "true" colloids, ThO_2(am, aged), precipitated with colloids by sweep flocculation (Figure 3.4). The saturation index of Th(IV) oxides calculated by Visual MINTEQ in different concentration is shown in Table 3.2. ThO_2(cr) was assumed to be the primary precipitation according to the table, but no sediments

were discovered in samples of 0.5 mg/L and 1.0 mg/L. In addition, Neck and Kim (2001) stated that the equilibrium time for amorphous Th(IV) oxides to transform into the crystalline solid required 270 days at 25˚C and about 12 days at 100˚C. Therefore, ThO_2(cr) was excluded and ThO_2(am, aged) was primarily taken into account when studying the potential source of precipitation in samples containing high concentration of Th(IV).

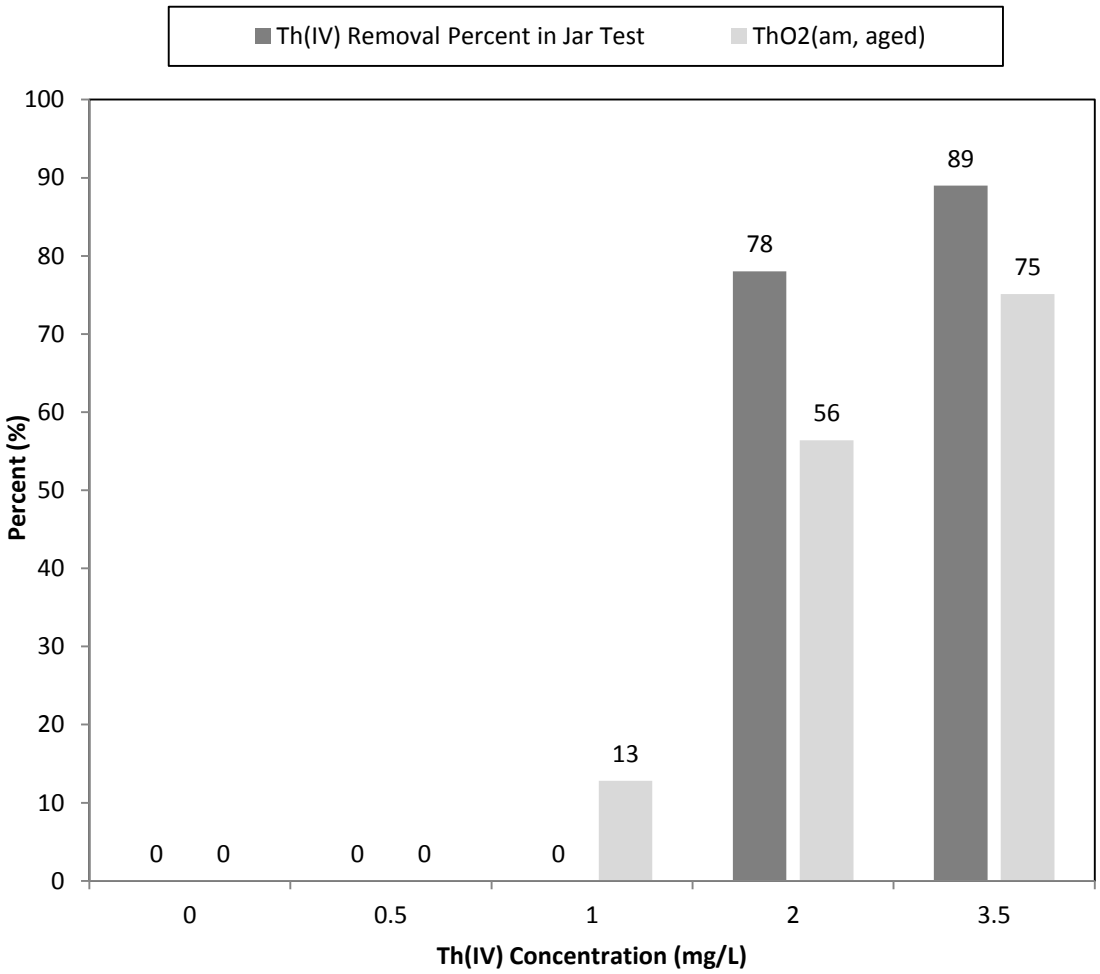

Figure 3.4: Percent removal of Th(IV) in jar test and potential formation of ThO_2(am, aged) calculated by Visual MINTEQ: dark color of columns indicates Th(IV) removal percent, and light color of columns indicates ThO_2(am, aged) formation.

Table 3.2: The saturation index (SI) of Th(IV) oxides for different concentrations of Th(IV) in pH of 4.0 and 0.001 M ionic strength, calculated by Visual MINTEQ.

	Saturation Index		
Th(IV) (mg/L)	ThO2(cr)	ThO2(am, aged)	ThO2(am, fresh)
0.5	6.494	-0.240	-1.040
1	6.734	0	-0.8
2	6.734	0	-0.8
3.5	6.734	0	-0.8

Note: SI < 0, solid in solution is undersaturated; SI = 0, solid in solution is equilibrium; SI > 0, solid in solution is oversaturated.

3.3.2 Kaolinite Transport in Saturated Sand Column in Absence of Th(IV)

Since kaolinite and Th(IV) influence each other, the behavior of kaolinite transport could be different when Th(IV) is present in one column. For comparison purpose, the first experiments were performed to determine the breakthrough of 100 mg/L kaolinite solution with 0.001 M $NaNO_3$ and a pH of 4.0 in a Th(IV)-free column.

Column experiment #1 was conducted by introducing a step input of 100 mg/L kaolinite solution with 0.001 M ionic strength and a pH of 4.0 in the sorption phase. The same background solution containing 0.001 M $NaNO_3$ at a pH of 4.0 was used later in the desorption phase. The result of 100 mg/L kaolinite transport alone is shown in Figure 3.5. The initial breakthrough of colloidal kaolinite was very similar to that of the conservative tracer bromide (Figure B.2), indicating the high mobility of colloids in saturated sand media. In addition, because colloidal suspension aggregated and attached to the solid phase by physical-chemical forces that is controlled by chemical, electrostatics, or van der Walls forces, causing the small and irreversible deposition of kaolinite onto sand grains, the plateau of the kaolinite curve did not reach to unity (Gao et al. 2006;

Kretzschmar and Schafer 2005; Saiers and Hornberger 1996). The maximum C/C_0 of kaolinite reached to 0.91 and the average recovery for duplicate Exp #1 was 87.9±0.4%.

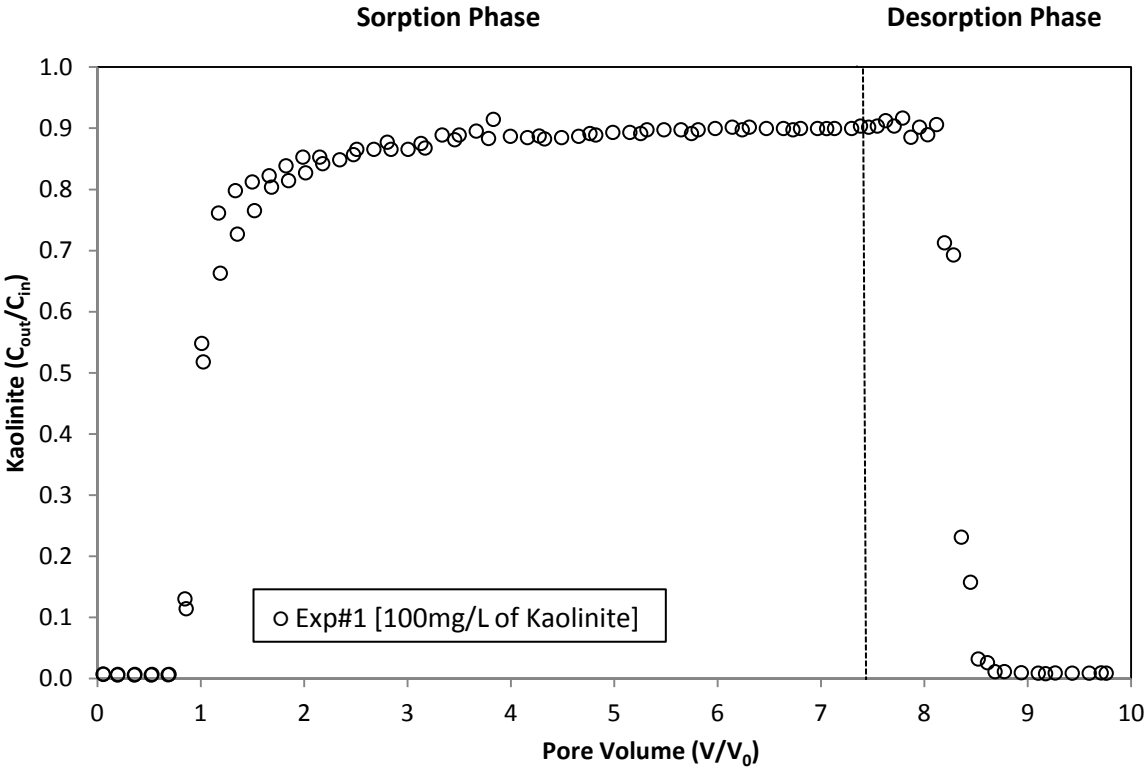

Figure 3.5: Effluent total kaolinite concentration in Exp #1 (data from duplicate transport experiments) in which 100 mg/L kaolinite transport through the saturated sand media in the absence of Th(IV) (pH=4.0, I=0.001 M, Temp=26±1°C, q=0.2 cm/min). Dotted line indicates changes from sorption phase to desorption phase.

3.3.3 Th(IV) Transport in Saturated Sand Column in Absence of Colloids

Column Exp #2 and Exp #3 were conducted to determine the behaviors of Th(IV) migration in colloid-free columns. Both of these column experiments had identical procedures but different concentration of Th(IV) in the sorption phase, performing 1.0 mg/L Th(IV) in Exp #2 (as shown in Figure 3.6) and 2.65 mg/L Th(IV) in Exp #3 (as shown in Figure 3.7). As seen from Figure 3.6 and Figure 3.7, the transport of Th(IV) within the column was highly retarded and both breakthrough curves had a long tail in

the desorption phase. The initial breakthrough did not occur until 1.0 mg/L Th(IV) solution transited 20 pore volumes (PVs) through the saturated porous media. The initial breakthrough curve of 2.65 mg/L Th(IV) took roughly 10 PVs to penetrate from the column, which was much different than the migration of 1.0 mg/L Th(IV). Except for the different PVs it took to reach breakthrough, these two curves have distinguishing shapes in that the 1.0 mg/L curve is more linear in both sorption and desorption phases, while the 2.65 mg/L curve is much smoother and parabolic in first phase and concave in second phase.

One interpretation for why the breakthrough of 1.0 mg/L Th(IV) required twice as many pore volumes as the 2.65 mg/L Th(IV) transport alone is that there exists maximum adsorption capacity for quartz sand to attach Th(IV), so the lower concentration of insoluble contaminant migrating in saturated sand media will lead to much more significant retardation. In addition, based on mass balance calculation, the initial breakthrough of Th(IV) occurred when the quartz sands in both columns adsorbed similar amounts of actinides (5.0 mg/kg Th(IV) in Exp #2, and 5.7 mg/kg Th(IV) in Exp #3). In addition, the average recovery of Exp #2 is $55.4 \pm 1.1\%$ and $82.3 \pm 1.3\%$ for Exp #3.

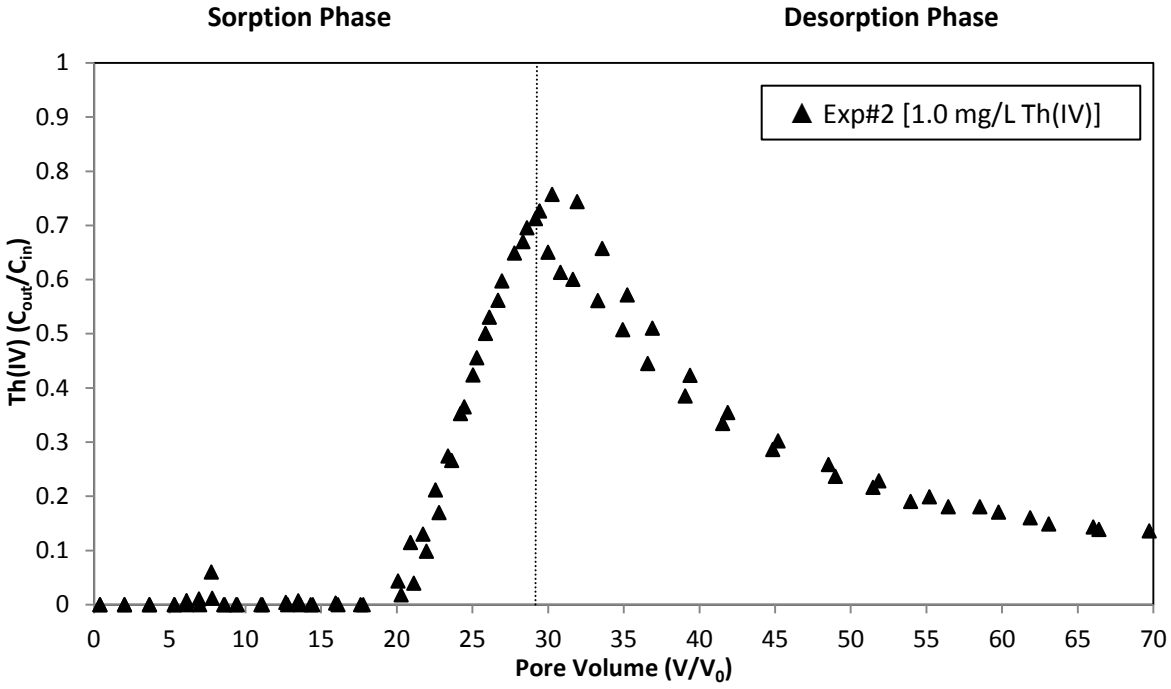

Figure 3.6. Effluent total Th(IV) concentration in Exp #2 (data from duplicate transport experiments) in which 1.0 mg/L Th(IV) transport through the saturated sand media in the absence of colloids (pH=4.0, I=0.001 M, Temp=26±1°C, q=0.2 cm/min). Dotted line indicates changes from sorption phase to desorption phase.

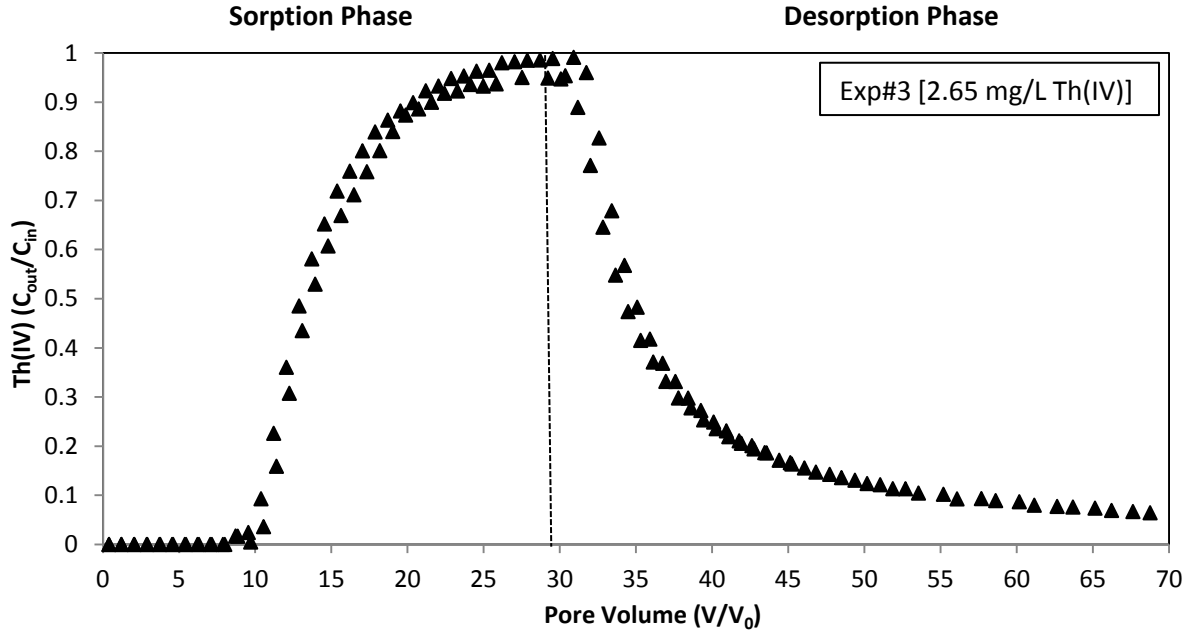

Figure 3.7. Effluent total Th(IV) concentration in Exp #3 (data from duplicate transport experiments) in which 2.65 mg/L Th(IV) transport through the saturated sand media in the absence of colloids (pH=4.0, I=0.001 M, Temp=26±1°C, q=0.2 cm/min). Dotted line indicates changes from sorption phase to desorption phase.

3.3.4 Transport of Colloidal Th(IV) in the Column Packed with Quartz Sands.

As mentioned earlier, many literatures suggest that colloids can be responsible for facilitating the transport of a variety of contaminants. Moreover, previous jar testing has demonstrated that 1 mg/L Th(IV) was capable of forming pseudo-colloids with 100 mg/L kaolinite, indicating the potential possibility that Th(IV) adsorbed on the surface of colloidal particles might mobilize along with kaolinite without any retardation in saturated porous media. In order to verify the possibility that whether kaolinite can enhance the transport of Th(IV) in the porous media, Exp #4 and Exp #5 were conducted. These two column experiments used mixtures of 100 mg/L kaolinite and two different concentrations of Th(IV) (1 mg/L and 2.65 mg/L) with 0.001 M ionic strength at a pH of 4.0 as influent solutions in sorption phase. Other conditions and procedures in these two experiments were consistent with Exp #2 and Exp #3.

The results of Exp #4 and Exp #5 are shown in Figure 3.8 and Figure 3.9, respectively. Figure 3.8 exhibited that the transport of 1.0 mg/L Th(IV) and 100 mg/L kaolinite has a similar shape to that of 100 mg/L kaolinite alone (Figure 3.5). The breakthrough of 1.0 mg/L Th(IV) in Exp #4 was essentially unretarded and almost occurred 20 times earlier compared to Exp #2 in which colloids were absent from the solution (Figure 3.6). Therefore, column Exp #4 successfully demonstrated that the pseudo-colloids were capable of migrating in the interstitial space between lager sandy particles like normal colloids. It also demonstrated that the adsorption capacity of kaolinite to Th(IV) is much greater than that of pure quartz to Th(IV) because there was barely retardation or interruption of Th(IV) transport in this experiment. Melson (2012) concluded that the stronger adsorption of Th(IV) onto clayey sediments (goethite and

kaolinite) was most possible because of the significantly larger BET (Brunauer-Emmett-Teller) surface area (15.31 m^2/g) in comparison to the sandy surface (1.27 m^2/g). The higher surface area, the more adsorption sites for particles could provide to contaminants. This adsorption for Th(IV) and colloidal kaolinite is assumed to be attributed to surface complexation reactions (Melson 2012).

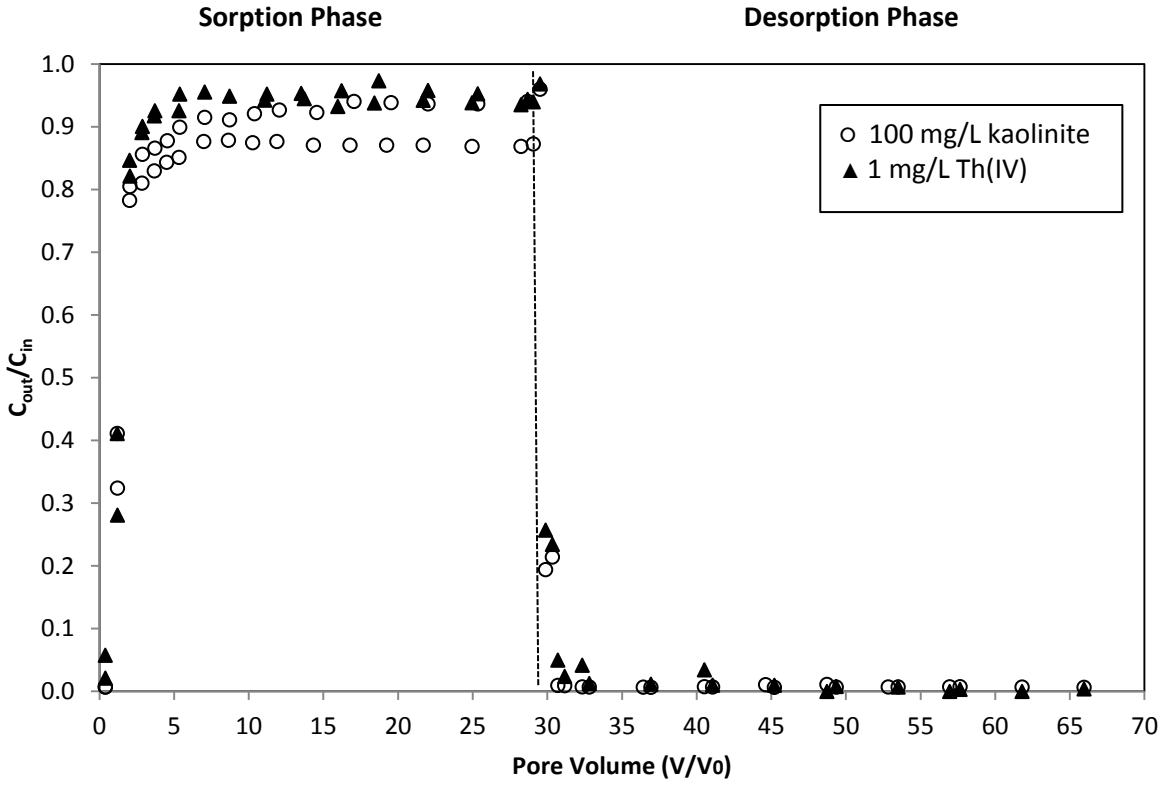

Figure 3.8. Effluent total kaolinite (100 mg/L) and Th(IV) (1 mg/L) mixture solution transport through the saturated sand media in Exp #4 (data from duplicate transport experiments): The open circles (○) indicate kaolinite concentration ratio, and the solid triangles (▲) indicate Th(IV) concentration ratio.

However, the mobilization of 100 mg/L kaolinite with 2.65 mg/L Th(IV) produced opposite results. As seen from Figure 3.9, all effluent samples contained neither kaolinite nor Th(IV), indicating that two substances were all retained within the column. Figure 3.10 showed that solids plugged the top PTFE frit (50 μm) used to prevent quartz

sands from going through with fluids. In addition, the influent solution consisting of Th(IV) and kaolinite mixtures reduced to 57% of the initial concentration after 35 PVs, which agreed with the result of jar testing that higher concentration of Th(IV) ($\geq$ 2 mg/L) with 100 mg/L kaolinite caused dramatically coagulation and precipitation in the end. Due to the strong aggregation between actinides and colloids, large molecular complexes were created during the transport process in the column, and eventually filtered from conducting fluid by physical straining or blocked by PTFE frit. Therefore, from the results of Exp #4 and Exp #5, it could be concluded that the colloid-facilitated transport would play a significant role in mobilizing Th(IV), only when the adsorption sites on colloidal kaolinite surfaces used to attach Th(IV) were undersaturated, which formed mobile pseudo-colloids. However, once the adsorption sites were equilibrium or oversaturated, the stability of colloids would be destroyed, and finally aggregated to large sediments due to coagulation. Hence, as high level of actinides and colloids were co-transporting in sand media, filtration process of Th(IV)-kaolinite compounds from conducting fluids by pores between sandy particles will be the predominant behavior for them.

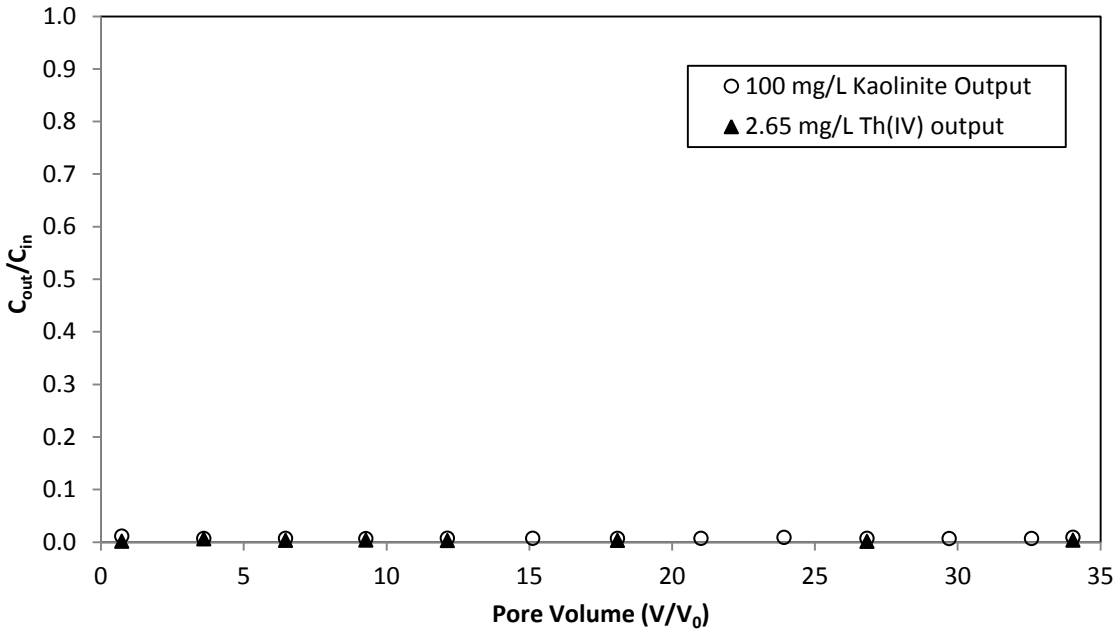

Figure 3.9. Effluent total kaolinite (100 mg/L) and Th(IV) (2.65 mg/L) mixture solution transport through the saturated sand media in Exp #5: The open circles (○) indicate kaolinite concentration ratio, and the solid triangles (▲) indicate Th(IV) concentration ratio. Note: the final influent concentrations of kaolinite and Th(IV) in this column experiment were decreased to 57% of initial concentration.

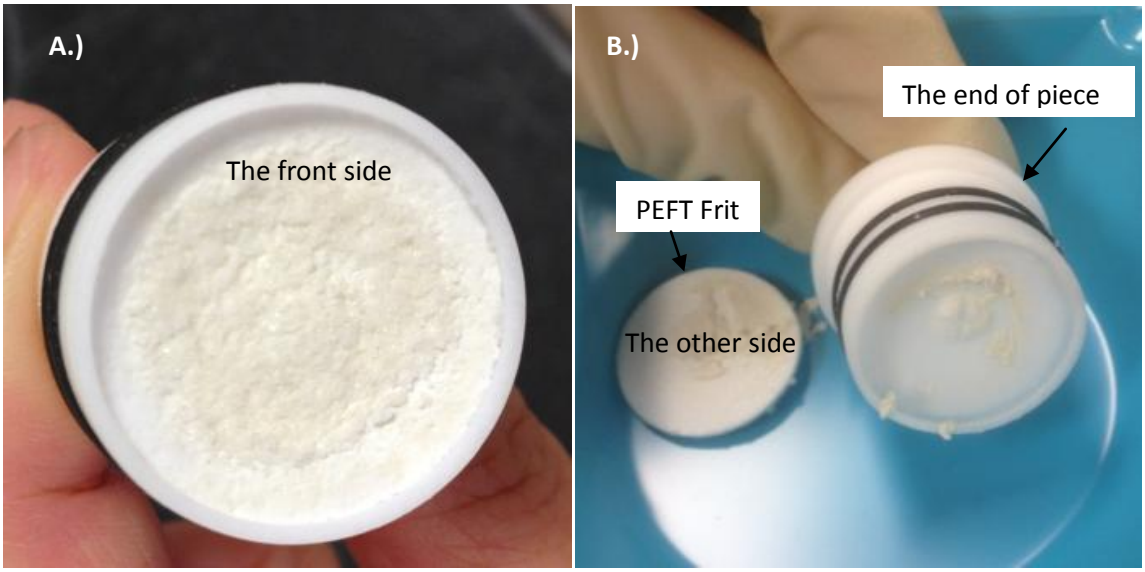

Figure 3.10. Precipitation of colloidal kaolinite and Th(IV) compounds blocked by 50 μm diameter frit at the top of end piece (outlet) in Exp #5. Picture A: frit is inside the end piece; Picture B: frit was removed from the end piece.

3.3.5 Transport of Th(IV) when Kaolinite Present in Saturated Porous Media.

Figure 3.8 has demonstrated that pseudo-colloids of 1 mg/L Th(IV) and 100 mg/L kaolinite could transport without any retardation in saturated sand media. However, the pseudo-colloids were produced before they migrate into columns. Hence, the following two experiments were performed to examine whether the transport of Th(IV) could be enhanced by colloidal kaolinite as well when they are introduced into column separately, which means that whether kaolinite transport can stripe Th(IV) off from sand surface and co-transport with it like pseudo-colloids. Figure 3.11 and Figure 3.12 showed the results of Exp #6 (1 mg/L Th(IV)) and Exp #7 (2.65 mg/L Th(IV)) with kaolinite input into column first, and then Th(IV), and finally kaolinite again. In Phase I, 100 mg/L kaolinite transports in both experiments were in agreement, and both recoveries in this phase were 91% (~ 9% of kaolinite entrapped in column at the end of Phase I). In Phase II, the initial breakthroughs of 1 mg/L Th(IV) (21 PVs) and 2.65 mg/L Th(IV) (11 PVs) (The initial of breakthrough start counting from the beginning of Phase II) was roughly close to that of Th(IV) transported at colloid-free columns shown in Figure 3.6 and Figure 3.7, indicating that the small amount of kaolinite deposited onto quartz sands in Phase I played a negligible role in Th(IV) transport. However, these small kaolinite could be liberated by Th(IV) transport. Based on mass balance, there were 38% and 45% of kaolinite released in Exp #6 and Exp #7, respectively. This can be explained by the adsorption of Th(IV) expanding the electrostatic double layers of colloids and reversing its negative surface charge (Haliena 2012; Sen and Khilar 2006).

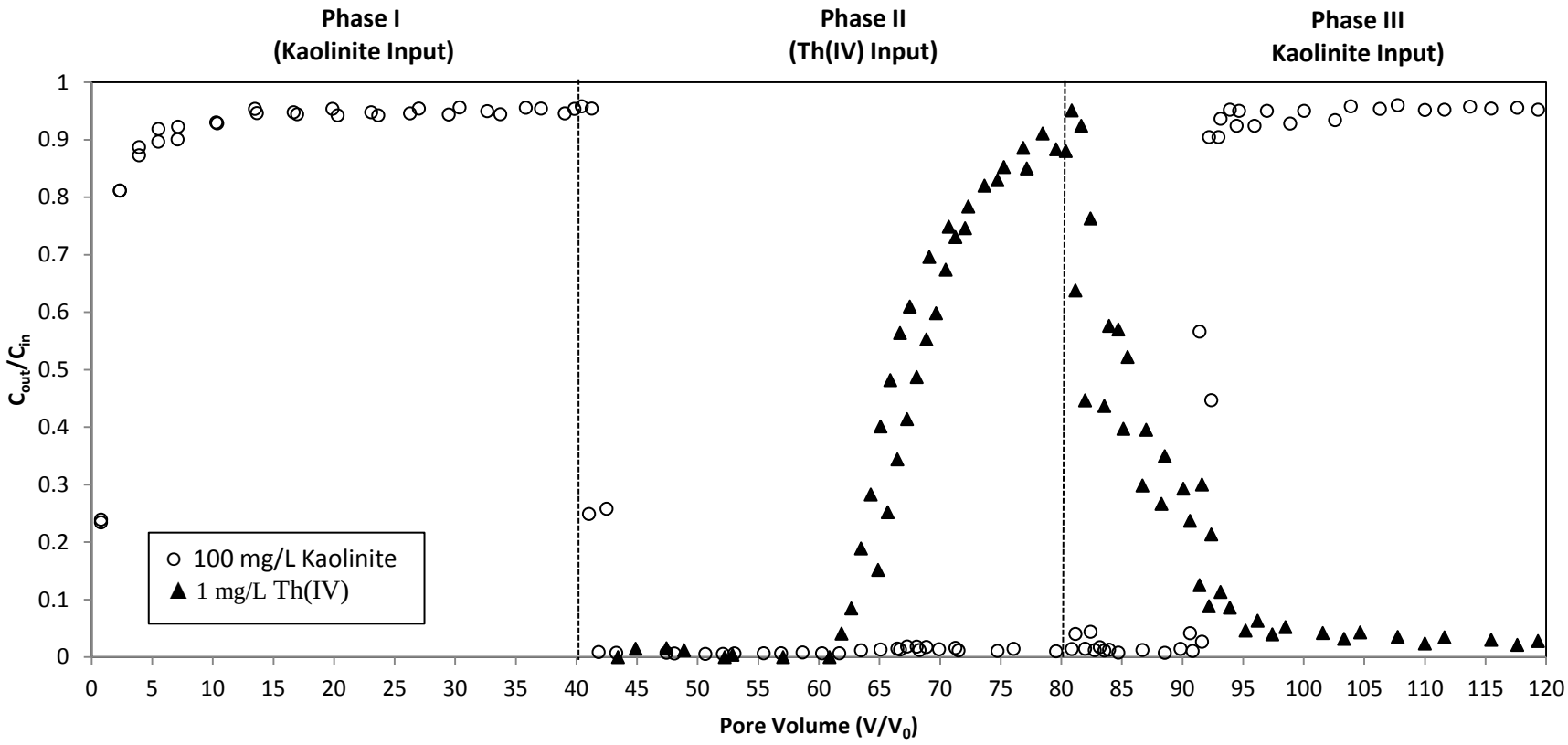

Figure 3.11: Effluent total kaolinite (○) and Th(IV) (▲) concentration in Exp #6 (data from duplicate transport experiments) in which 1 mg/L Th(IV) transport through the column under 100 mg/L kaolinite as background solution (pH=4.0, I=0.001 M, Temp=26±1°C, q=0.2 cm/min). Dotted lines indicate changes of different input solutions.

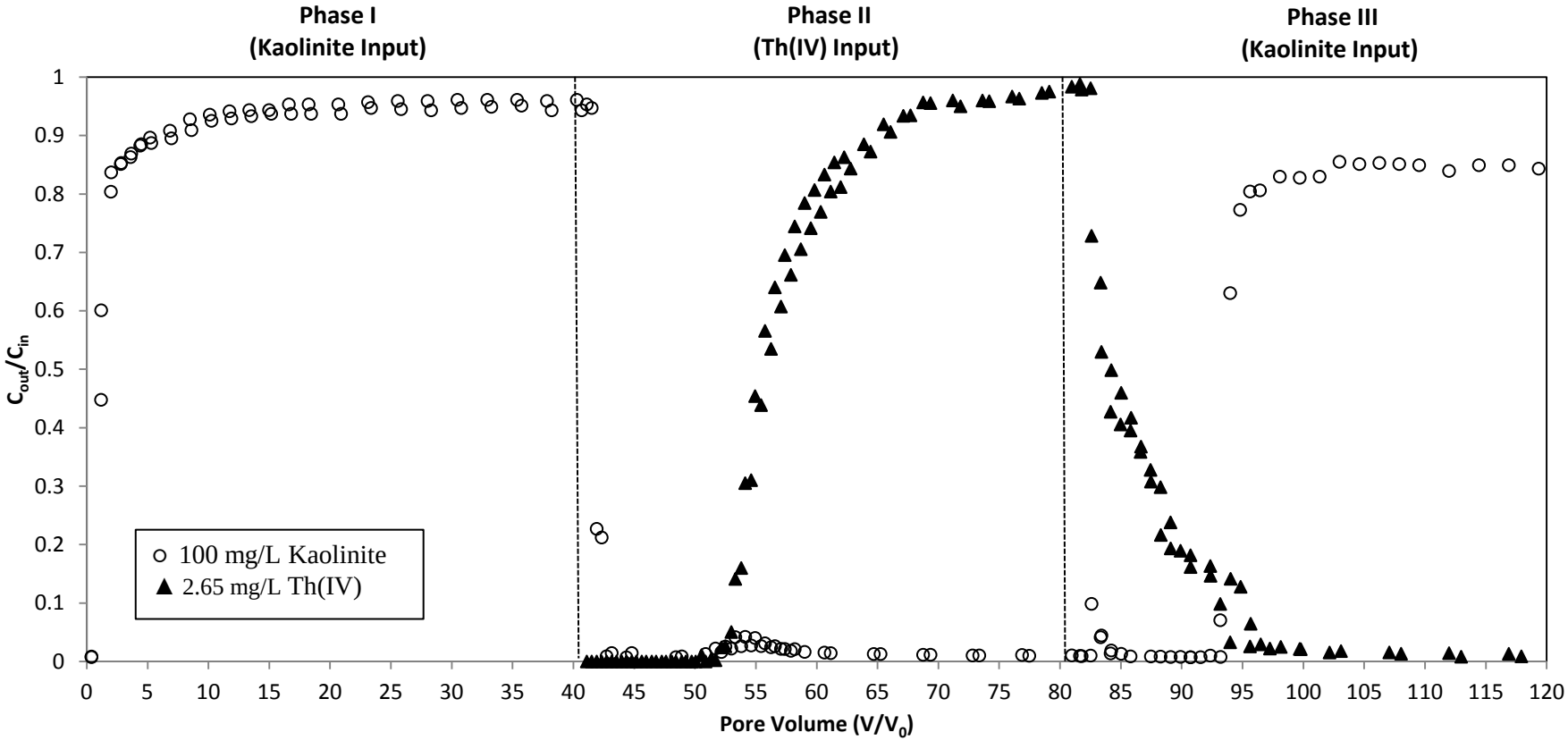

Figure 3.12: Effluent total kaolinite (○) and Th(IV) (▲) concentration in Exp #7 (data from duplicate transport experiments) in which 2.65 mg/L Th(IV) transport through the column under 100 mg/L kaolinite as background solution (pH=4.0, I=0.001 M, Temp=26 ±1°C, q=0.2 cm/min). Dotted lines indicate changes of different input solutions.

In Phase III for Th(IV) desorption from sand grains, the prolong tail disappeared, replaced by a zigzag curve. The sharp decreased Th(IV) desorption from sand surface occurred as turbidity started increasing in effluent samples. Due to the size exclusion effect, few kaolinite appeared around 1 pore volume. However, the real breakthrough of colloids in Phase III for both experiments showed much more significant retardation compared to Phase I where kaolinite migrate in uncontaminated porous media (Figure 3.13 and Figure 3.14): roughly 10 PVs in Exp #6 in which 5.5 mg kaolinite and 0.68 mg Th(IV) were sorbed onto 93 g of sands at Phase I and Phase II (equivalent 59 mg/kg kaolinite and 7.3 mg/kg Th(IV), and 12 PVs in Exp #7 in which 4.73 mg kaolinite and 1.15 mg Th(IV) were sorbed onto 92 g of sands (equivalent 51 mg/kg kaolinite and 12.5 mg/kg Th(IV)). Surface complexation reaction between Th(IV) and kaolinite may help explain the great retention of colloids transport. Sun (2010) examined the dynamics of kaolinite and lead (Pb) in the saturated porous media and also found that the presence of Pb on colloid surface and sand grain surface can reduce the mobilization of kaolinite. Moreover, Figure 3.13 have shown that the plateau of kaolinite transport in Phase I and Phase III were identical (the maximum C/C_0 was at 0.94) and recovery kept 91%, while the plateau of kaolinite transport at Phase III in Figure 3.14 only reached around 0.8 and the recovery reduced to 68% from 91%. Therefore, the presence of Th(IV) on sand media definitely decelerated colloidal kaolinite mobility and higher concentration of the actinide caused greater decrease of colloid recovery.

As concluded previously, the affinity of insoluble contaminant to colloid was stronger than to quartz sand attributed to its larger surface area, so it was assumed that colloids could scavenge Th(IV) that already adsorbed onto the sand surface, and facilitate

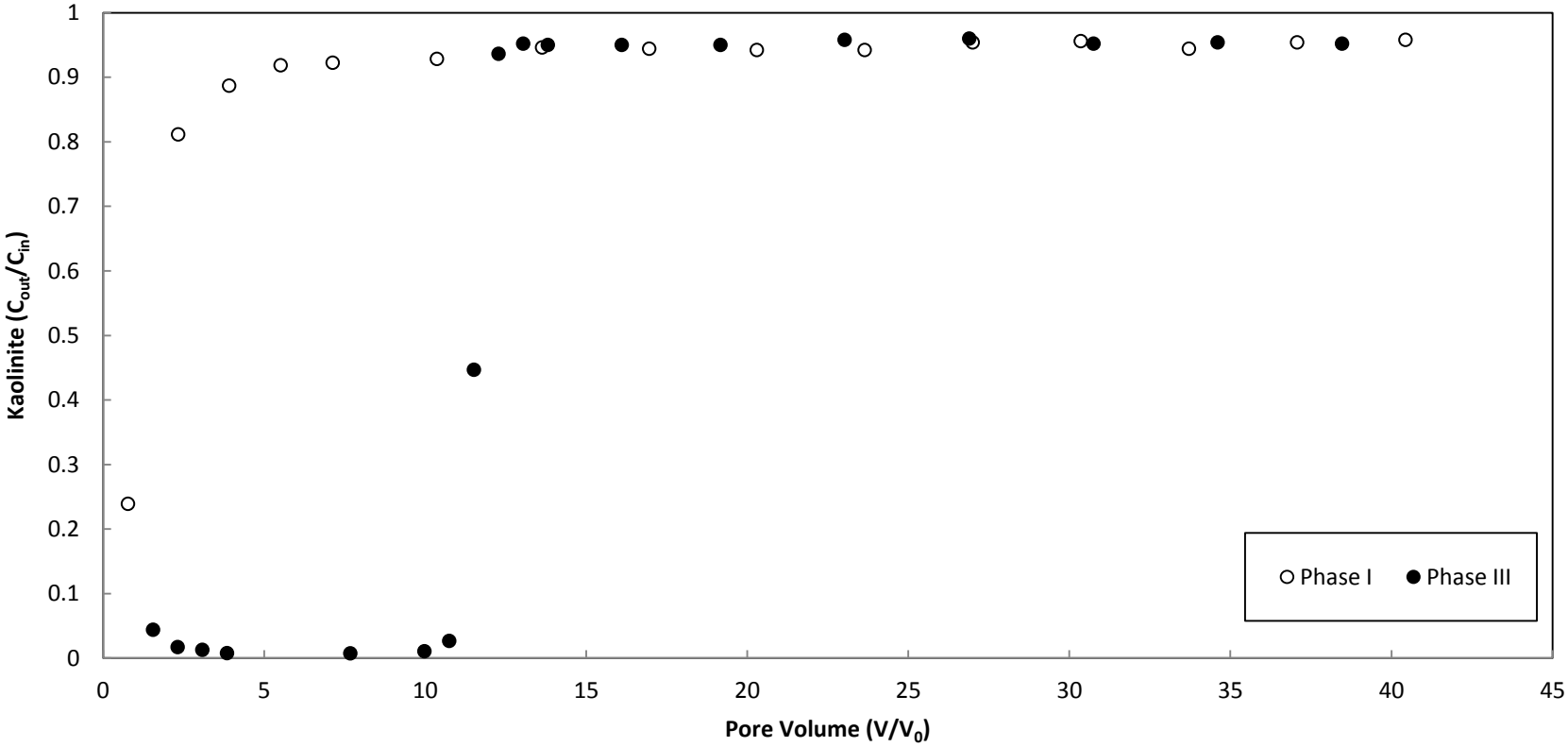

Figure 3.13: Comparison breakthroughs of kaolinite transport between Phase I and Phase III in Exp #6 (Whole plot is in Figure 3.11): The open circles (○) indicate kaolinite breakthrough in Phase I, and the solid circles (●) indicate kaolinite breakthrough in Phase III (equivalent 59 mg/kg kaolinite and 7.3 mg/kg Th(IV) were retained in the column after Phase I and Phase II).

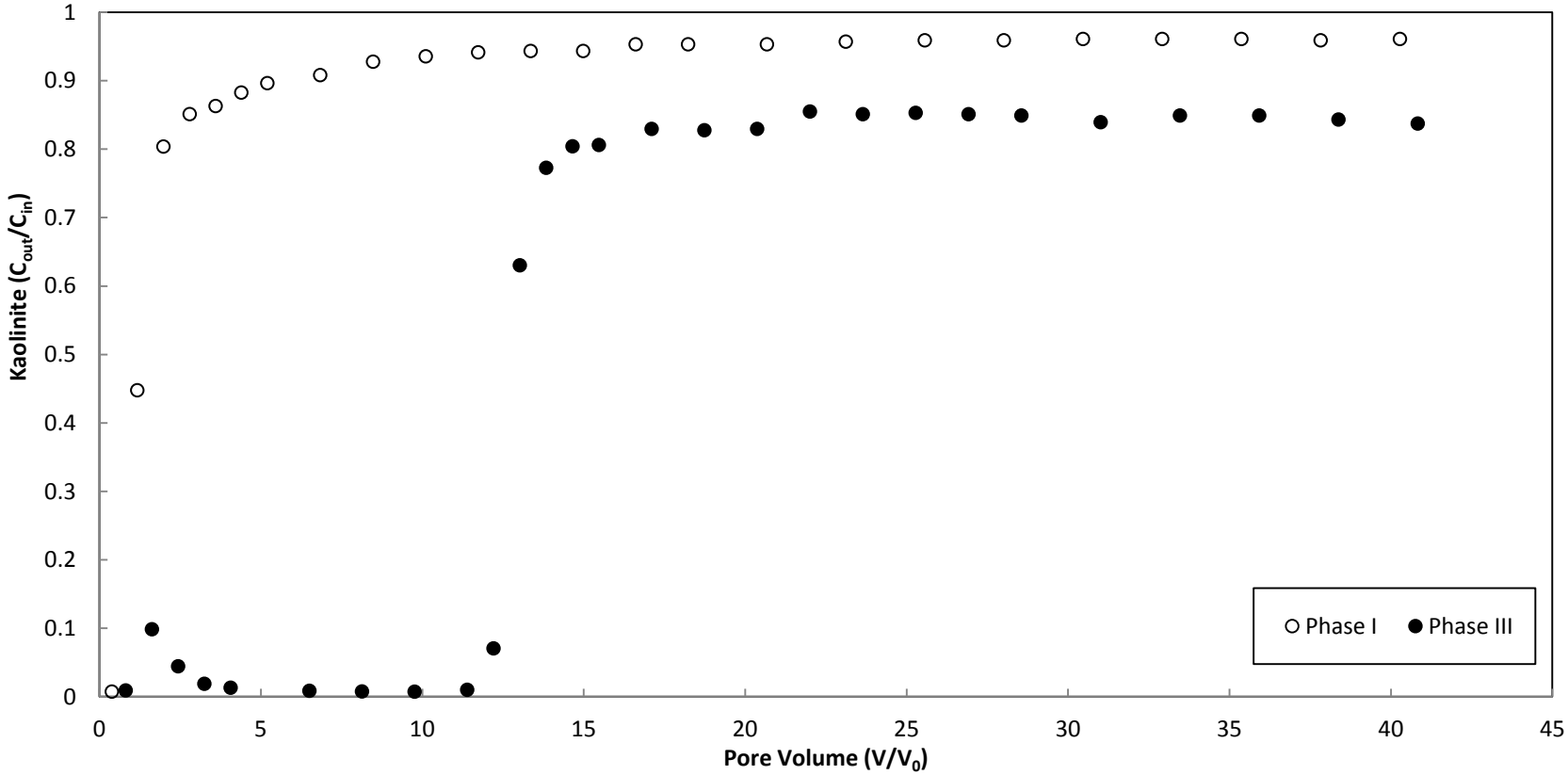

Figure 3.14: Comparison breakthroughs of kaolinite transport between Phase I and Phase III in Exp #7 (Whole plot in Figure 3.12): The open circles (○) indicate the breakthrough of kaolinite in Phase I, and the solid circles(●) indicate the breakthrough of kaolinite in Phase III (equivalent 51 mg/kg kaolinite and 12.5 mg/kg Th(IV) were retained in the column after Phase I and Phase II).

its transport (Sun et al. 2010). For instance, Zhu et al (2012) discovered that mobile colloidal kaolinite was capable of stripping adsorbed mercury (Hg) off from sand matrix and enhancing Hg transport as kaolinite started breaking through, and both kaolinite and Hg concentration reached a close peak within 1.5 PV. However, kaolinite migration did not trigger the release of Th(IV) from sands in this study. As seen from Figure 3.11 and Figure 3.12, Th(IV) concentration only decreased sharply within 10 PVs, and did not increase at all in the whole process of Phase III. This outcome may be because Th(IV) and kaolinite at Phase II and at the start of Phase III had complexation reaction to form large particles entrapped in columns by multiparticle bridging. In other words, Th(IV) might has been adsorbed on the surface of colloids not sands before kaolinite breakthrough. Therefore, Exp #6 and Exp #7 demonstrated that due to the strong adsorption of Th(IV), kaolinite transport could happen drastic retardation in the sand media even containing little Th(IV), and it did not scavenge Th(IV) from pore surface or formed to mobile pseudo-colloids. These two experiments also demonstrated that the adsorption process between strongly sorbing contaminants and colloids are irreversible so that new kaolinite passing through the saturated porous media cannot attach Th(IV) anymore which has already bound with old colloids.

3.3.6 Transport of Kaolinite when Th(IV) Present in the Saturated Porous Media

Exp #6 and Exp #7 demonstrated that kaolinite could not enhance Th(IV) transport when the actinide retained in columns due to formation compounds with colloids, and Th(IV) transport was capable of liberating small amounts of kaolinite entrapped in sand media owing to physical-chemical collections between colloids and sands matrix. Therefore, the next Exp #8 (1 mg/L Th(IV)) and Exp #9 (2.65 mg/L Th(IV))

were conducted to verify whether kaolinite could accelerate Th(IV) mobility when it was only adsorbed onto sand surface, and to examine the effect of kaolinite deposition on Th(IV) migration. These two experiments had identical conditions (pH=4.0 and I=0.001 M) and procedures but different sequence of influent solutions (input Th(IV) first, and then kaolinite, finally Th(IV) again) than Exp #6 and Exp #7.

Figure 3.15 and Figure 3.16 showed the results of Exp #8 and Exp #9, respectively. In Phase I, the breakthrough of Th(IV) (20 PVs for 1 mg/L Th(IV), 10 PVs for 2.65 mg/L Th(IV)) was consistent with that in Exp #2 and Exp #3 in which Th(IV) transport in colloid-free saturated quartz sands (Figure 3.6 and Figure 3.7). In Phase II, when 100 mg/L kaolinite transport right after Th(IV) migration in quartz sands, the behaviors of Th(IV) in both experiments were similar, such as the rapid decline of Th(IV) concentration during the first 10 PVs, Th(IV) disappearance in the effluent samples as the colloids reached high concentration (approximately 0.9 C/C_0), and significant retardation of kaolinite transport. Moreover, Phase II in Exp #8 and Exp #9 was almost corresponding with Phase III in Exp #6 and Exp #7. Likewise, Th(IV) concentration did not increase with colloidal kaolinite mobilization. This observation indicated that kaolinite did not successfully stripe Th(IV) off from sand surface. In Phase III, the breakthrough of 1 mg/L Th(IV) was detected approximately at 40 PVs in Exp #8 in which 93.57 g quartz sands held 28.24 mg kaolinite (equivalent 302 mg/kg) and 0.45 mg Th(IV) (equivalent 5 mg/kg). The high concentration of Th(IV) breakthrough was occurred roughly at 20 PVs in Exp #9 in which 93.50 g quartz sands contained 31.75 mg kaolinite (equivalent 340 mg/kg) and 0.56 mg Th(IV) (equivalent 6 mg/kg). Figure 3.17 and Figure 3.18 directly exhibited that Th(IV) migrations reduced roughly twice in Phase

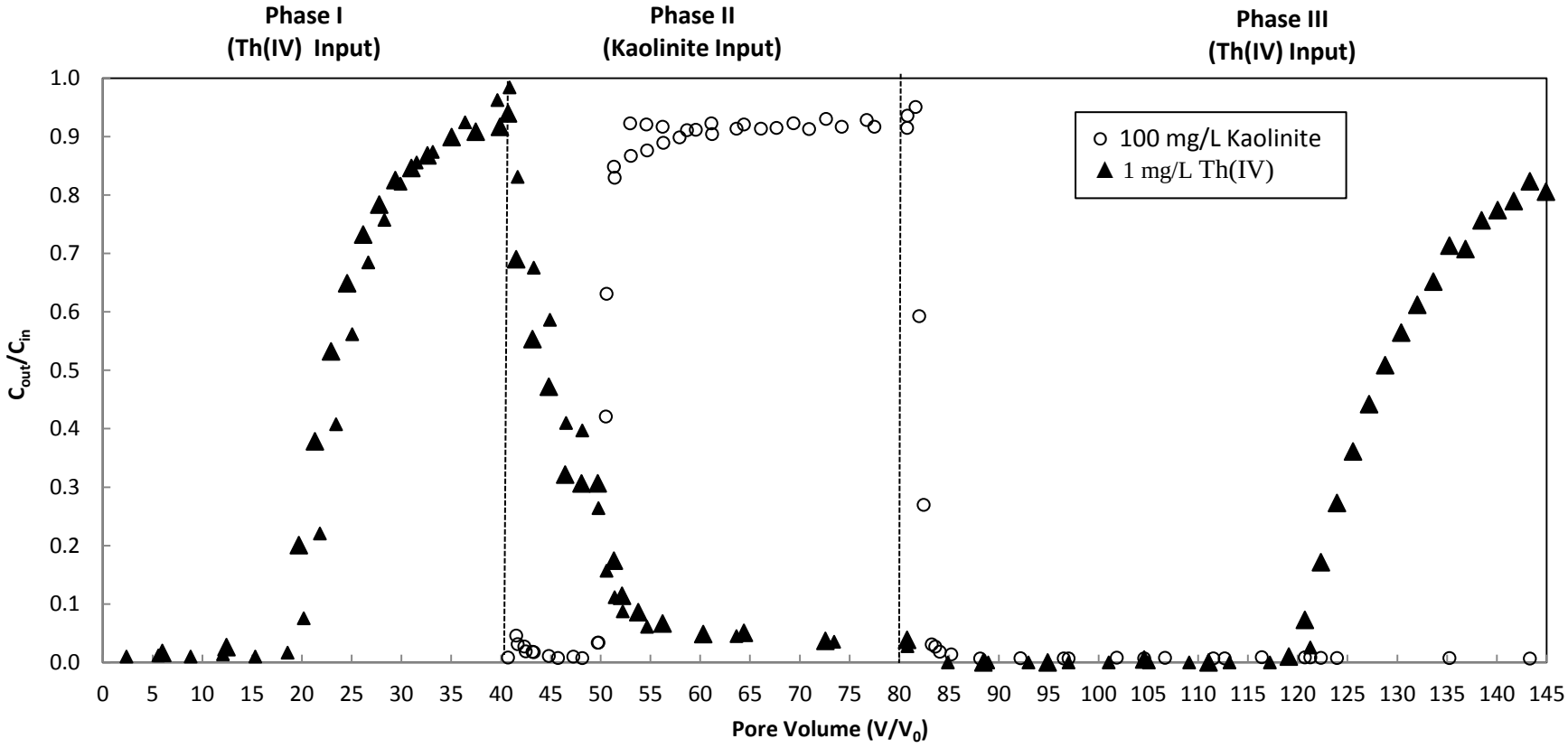

Figure 3.15: Effluent total Th(IV) (▲) and kaolinite (○) concentration in Exp #8 (data from duplicate transport experiments) that 1 mg/L Th(IV) transport through the column packed with pure quartz sand disturbed by 100 mg/L kaolinite (pH=4.0, I=0.001 M, Temp=26 ±1°C, q=0.2 cm/min). Dotted lines indicate changes of different phases.

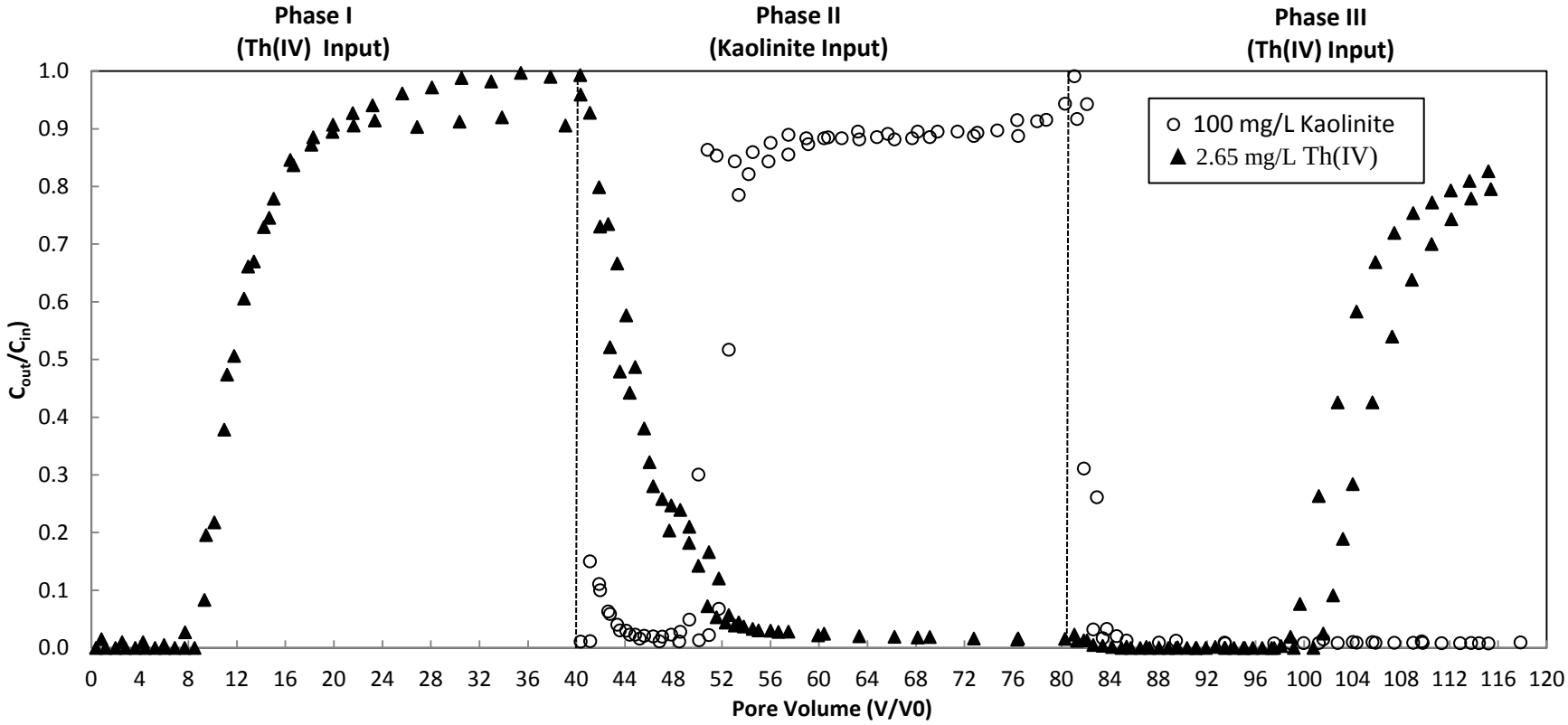

Figure 3.16: Effluent total Th(IV) (▲) and kaolinite (○) concentration in Exp #9 (data from duplicate transport experiments) that 2.65 mg/L Th(IV) transport through the column packed with pure quartz sand disturbed by 100 mg/L kaolinite (pH=4.0, I=0.001 M, Temp=26±1°C, q=0.2 cm/min). Dotted lines indicate changes of different input solutions or phases.

III (Th(IV) adsorption onto both sands and kaolinite) than in Phase I (Th(IV) adsorption only onto sands). Therefore, the small accumulation of colloidal kaolinite in quartz sands is capable of increasing the retardation of Th(IV) transport due to higher adsorption capacity of kaolinite for Th(IV) over quartz sands. However, no turbidity was detected at Phase III in both experiments as Th(IV) broke through the column, which differed from the previous results that Th(IV) migration could release small irreversible colloidal kaolinite entrapped in sand media. As mentioned earlier, the surface complexation reaction led to kaolinite deposition in Phase II. Therefore, it can be concluded that Th(IV) only enhances the transport of colloidal kaolinite retained in the sands due to physical-chemical collection with sand grains not physicochemical deposition with other strong sorbing ions. The last two experiments demonstrated that when colloids and the actinide occurred in sand media separately, both breakthroughs would significantly retard due to high affinity of Th(IV) to kaolinite.

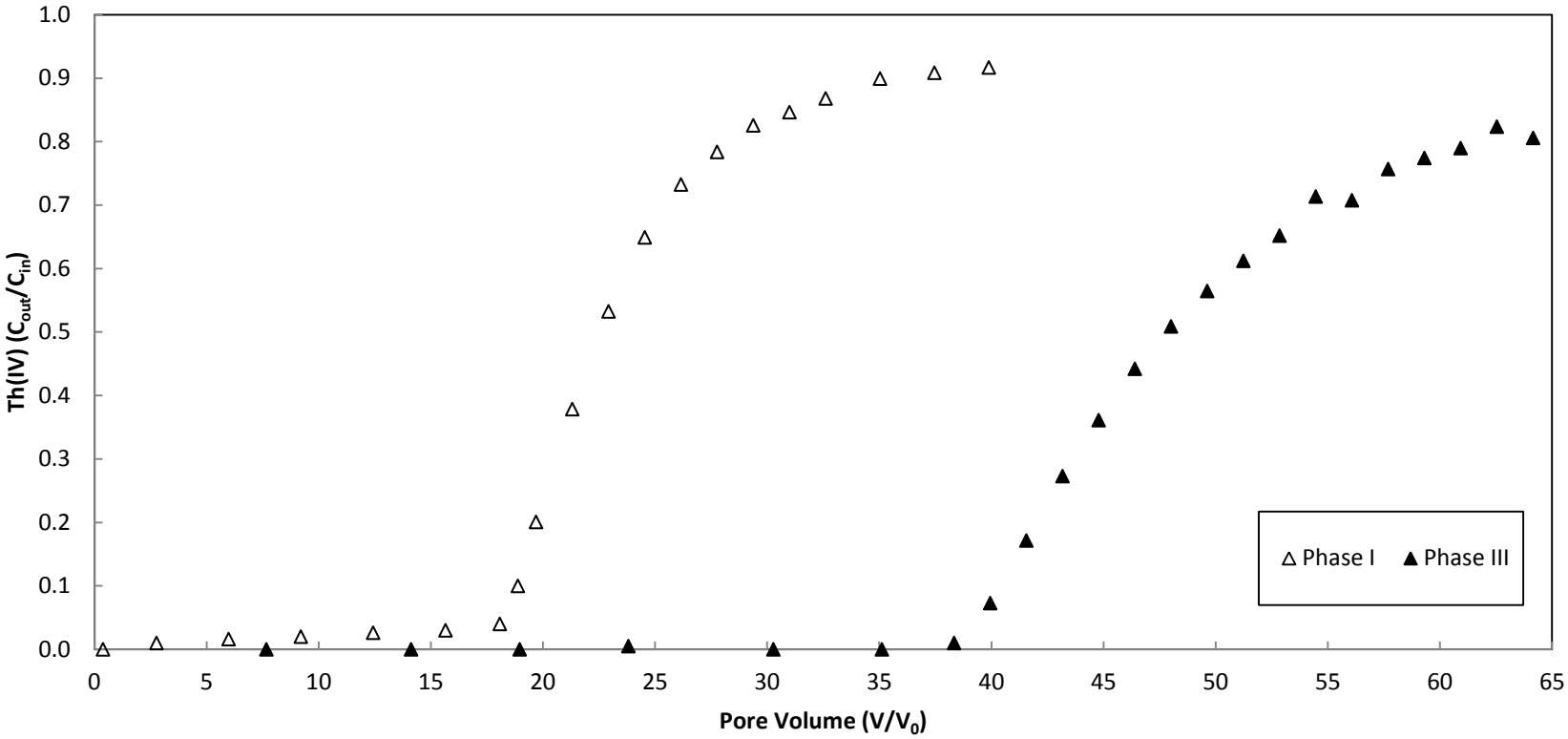

Figure 3.17: Comparison breakthroughs of 1 mg/L Th(IV) transport between Phase I and Phase III in Exp #8 (Whole plot is Figure 3.15): The open triangles (Δ) indicate Th(IV) breakthrough in Phase I, and the solid triangles (▲) indicate Th(IV) breakthrough in Phase III (equivalent 302 mg/kg kaolinite and 5 mg/kg Th(IV) were retained in the column after Phase I and Phase II).

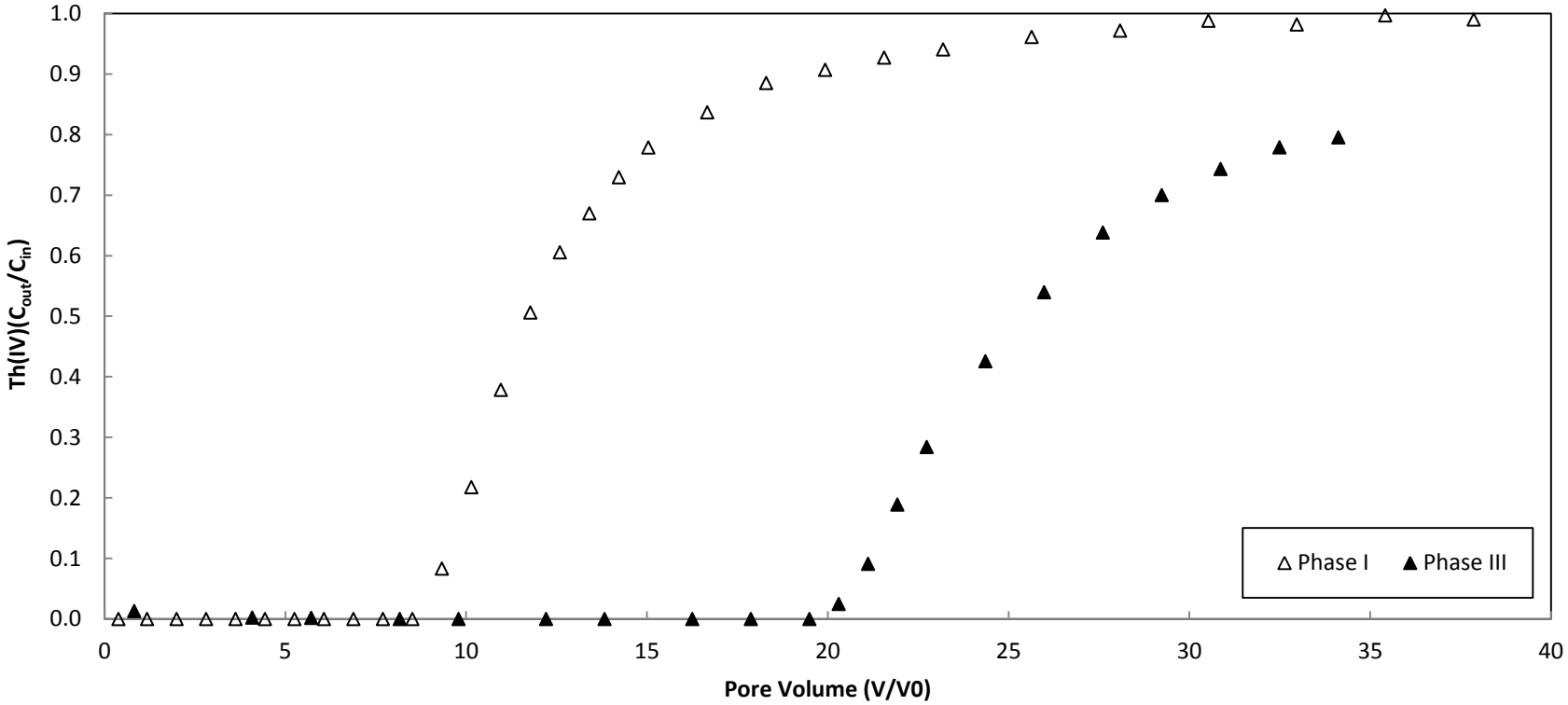

Figure 3.18: Comparison breakthroughs of 2.65 mg/L Th(IV) transport between Phase I and Phase III in Exp #9 (Whole plot is Figure 3.16): The open triangles (Δ) indicate Th(IV) breakthrough in Phase I, and the solid triangles (▲) indicate Th(IV) breakthrough in Phase III (equivalent 340 mg/kg kaolinite and 6 mg/kg Th(IV) were retained in the column after Phase I and Phase II).

Conclusions and Recommendations

4.1 Conclusions

Jar Test

1. ≤ 1 mg/L Th(IV) was capable of forming pseudo-colloids with 100 mg/L kaolinite, which indicated the possibility of colloid-facilitated transport of Th(IV), and larger than 2 mg/L Th(IV) occurred significantly coagulation and flocculation with 100 mg/L kaolinite, causing at least 80% turbidity and actinide removal.

Transport Alone

2. When 100 mg/L colloidal kaolinite with 0.001 M ionic strength at a pH of 4.0 migrated the saturated column packed only with quartz sands, it took approximately one pore volume (PV) to break through, and reached to maximum C/C_0 of 0.91 attributed to small and irreversible deposition of colloids onto the solid phase. The transport of kaolinite was much similar to that of conservative tracer bromides, indicating high mobility of kaolinite suspension. Moreover, the small irreversible deposition of kaolinite onto the sand grains, attributed to aggregation and attachment of colloidal kaolinite to quartz sands by physical-chemical forces, resulted in the plateau of the curve not reaching to unity.

3. For the transport of Th(IV) in saturated colloid-free column, the breakthroughs of actinides exhibited drastic retardation: 20 PVs for 1 mg/L Th(IV) and 10 PVs for

2.65 mg/L Th(IV). The breakthrough of 1.0 mg/L Th(IV) required twice as many pore volumes as the 2.65 mg/L Th(IV) transport, suggesting that there exists maximum adsorption capacity for quartz sand to bind with Th(IV). Consequently, the lower concentration of Th(IV) moving in sand media absent of colloids will take more pore volumes to fill up all available sorption sites on sands surface. Moreover, two Th(IV) transport curves were totally distinguishing that 1.0 mg/L Th(IV) transport is much more linear in both sorption and desorption phases, while the 2.65 mg/L Th(IV) transport is smoother and parabolic in first phase and concave in second phase.

Colloid-Facilitated Transport

4. The breakthrough of 1 mg/L Th(IV) adsorbed on 100 mg/L kaolinite was essentially unretarded, indicating that pseudo-colloids were capable of migrating insoluble contaminants in the interstitial space between lager sandy particles. In addition, kaolinite had stronger binding strength than sands because there was barely retardation or interruption of Th(IV) transport in this experiment. However, huge retention occurred when 2.65 mg/L Th(IV) and 100 mg/L kaolinite mixture migrated into column. Therefore, stable colloidal kaolinite can provide potentially pathways for Th(IV) transport. Nevertheless, it serves as a contaminant carrier only under the condition that the strong sorbing ions and colloids form mobile pseudo-colloids.

Colloid-Retardant Transport

5. When kaolinite was present in saturated sand media, the transport of Th(IV) spent more pore volumes to breakthrough on the basis of the retardation caused by adsorption only onto quartz sands. For example, both Th(IV) migrations retarded approximately twice in sand media containing 5 mg/kg Th(IV) and 302 mg/kg kaolinite for 1 mg/L Th(IV) transport, and 6 mg/kg Th(IV) and 340 mg/kg kaolinite for 2.65 mg/L Th(IV) transport. Therefore, the small kaolinite accumulation is capable of increasing retardation of the transport of Th(IV) due to higher affinity of kaolinite for Th(IV) over quartz sands.
6. Moreover, Th(IV) existence in quartz sands influence kaolinite migration as well that 6.5 or 9.3 mg/kg Th(IV) retained within columns caused approximately 10 times retardation of kaolinite transport compared to it mobilize alone in uncontaminated porous media. It may be explained that Th(IV) attracted mobile kaolinite to form large compounds, and due to multiparticle bridging, colloids were filtered from liquid phase by porous media.
7. In experiments that kaolinite and Th(IV) introduced to columns separately to investigate whether the higher Th(IV) adsorption affinity to kaolinite than sand particles may enable colloids to desorb the actinide from sand surface, the concentration of Th(IV) did not increase during colloids passing by, no matter where Th(IV) was adsorbed (only onto sands or onto both sands and colloids). However, kaolinite transport diminished Th(IV) desorption process which used to be prolonged, but now could be finished as kaolinite broke through (10~12 PVs). Surprisingly, Th(IV) transport was capable of enhancing kaolinite release from

quartz sands, but only for colloids deposited in porous media due to physical-chemical forces. This result might be owing to adsorption of Th(IV) altering colloids surface charge, increasing the double layer electrostatic repulsive forces between colloids and sandy particles.

Overall Conclusion

8. Kaolinite is capable of accelerating Th(IV) transport only when they form mobile pseudo-colloids. Once colloids and actinides transport separately, kaolinite cannot stripe Th(IV) off from pore surface and enhance its transport. Small deposition of kaolinite onto sand media caused significant retardation of Th(IV) transport attributed to increasing the accessibility of adsorption sites for Th(IV), and vice versa. Kaolinite accumulated in porous media by physical-chemical collections was released by high concentration of Th(IV) mobilization.

4.2 Recommendations for Future Works

1. Future column experiments studying colloid-associated transport of Th(IV) could use unsaturated condition to compare the results in saturated condition.
2. Future colloid-associated transport experiments also could study the influence of different flow rate causing different water content in sand media on the co-transport of Th(IV) and kaolinite (Th(IV) adsorbed onto colloids).

References

About.Com (2013). "Black/White Periodic Table." Chemistry, From http://chemistry.about.com/od/periodictables/ig/Printable-Periodic-Tables/Black-White-Periodic-Table.htm.

Ahearne, J. F. (1997). "Radioactive Waste: The Size of the Problem." *Physics Today*, 50(6), 24.

Altmaier, M., Neck, V., Denecke, M. A., Yin, R., and Fanghanel, T. (2006). "Solubility of ThO_2 center dot xH(2)O(am) and the formation of ternary Th(IV) hydroxide-carbonate complexes in $NaHCO_3$-Na_2CO_3 solutions containing 0-4 M NaCl." *Radiochimica Acta*, 94(9-11), 495-500.

Altmaier, M., Neck, V., and Fanghanel, T. (2004). "Solubility and colloid formation of Th(IV) in concentrated NaCl and $MgCl_2$ solution." *Radiochimica Acta*, 92(9-11), 537-543.

Altmaier, M., Neck, V., Müller, R., and Fanghänel, T. (2005). "Solubility of ThO_2 center dot xH(2)O(am) in carbonate solution and the formation of ternary Th(IV) hydroxide-carbonate complexes." *Radiochimica Acta*, 93(2), 83-92.

Anna-Maria, J. (1999). "Measurement and Modeling of Th Sorption onto TiO_2." *ournal of Colloid and Interface Science*, 220(2), 367-373.

ATSDR (1990). Toxicological Profile for Thorium, Agency for Toxic Substances and Disease Registry U.S. Public Health Service.

ATSDR (2011). "Detailed Data Table for the 2011 Priority List of Hazardous Substances.", Substance Priority List Retrieved January 19, 2012, from http://www.atsdr.cdc.gov/spl/resources/ATSDR_2011_SPL_Detailed_Data_Table.pdf.

Baes, C. F., Meyer, N. J., and Roberts, C. E. (1965). "The Hydrolysis of Thorium(IV) at 0 and 95 °." *Inorganic Chemistry*, 4(4), 518-527.

Banik, N. L., Buda, R. A., Bürger, S., Kratz, J. V., and Trautmann, N. (2007). "Sorption of tetravalent plutonium and humic substances onto kaolinite." *Radiochimica Acta*, 95(10), 569-575.

Barton, C. D., and Karathanasis, A. D. (2003). "Influence of soil colloids on the migration of atrazine and zinc through large soil monoliths." *Water Air and Soil Pollution*, 143(1), 3–21.

Bergendahl, J. A., and Grasso, D. (2003). " Mechanisc basis for parcle de- tachment from granular media." *Environmental Science & Technology*, 37, 2317–2322.

Bin, G., Cao, X., Dong, Y., Luo, Y., and Ma, L. Q. (2011). "Colloid Deposition and Release in Soils and Their Association With Heavy Metals." *Critical Reviews in Environmental Science and Technology*, 41(4), 336-372.

Bin, G., Xinde. Cao, Yan. Dong, Yongming. Luo, and Lena Q. Ma (2011). "Colloid Deposition and Release in Soils and Their Association With Heavy Metals." *Critical Reviews in Environmental Science and Technology*, 41(4), 336-372.

Brown, P. L., Ellis, J., and Sylva, R. N. (1983). "The hydrolysis of metal ions. Part 5. Thorium(IV)." *Journal of the Chemical Society, Dalton Transactions*(1), 31-34.

Bundschuh, T., Knopp, R., Müller, R., Kim, J. I., Neck, V., and Fanghänel, T. (2000). "Application of LIBD to the determination of the solubility product of thorium(IV)-colloids." *Radiochimica Acta*, 88((9-11_2000)), 625.

Burgisser, C. S., Cernik, M., Borkovec, M., and Sticher, H. (1993). "Determination of nonlinear adsorption isotherms from column experiment: An alternative to batch studies." *Environmental Science & Technology*, 27(5), 943-948.

Cantrell, K. J., and Riley, R. G. (2008). "Subsurface Behavior of Plutonium and Americium at Non-Hanford Sites and Relevance to Hanford, Pacific Northwest National Laboratory: PNNL-17386.".

Chen, C., and Wang, X. (2007). "Sorption of Th (IV) to silica as a function of pH, humic/fulvic acid, ionic strength, electrolyte type." *Applied Radiation and Isotopes*, 65(2), 155-163.

Chen, L., Yu, X. J., Zhao, Z. D., and Dong, Y. H. (2006). "The sorption of Th(IV) ions onto montmorillonite: the effect of pH, ionic strength and fulvic acid." *Adsorption Science & Technology*, 24(4), 301-310.

Choppin, G. R. (1999). "Utility of oxidation state analogs in the study of plutonium behavior." *Radiochimica Acta*, 85(3-4), 89-95.

Choppin, G. R. (2007). "Actinide speciation in the environment." *Journal of Radioanalytical and Nuclear Chemistry*, 273(3), 695-703.

Clark, D. L., Hobart, D. E., and Neu, M. P. (1995). "Actinide carbonate complexes and their importance in actinide environmental chemistry." *Chemical Reviews*, 95(1), 25-48.

Contardi, J. S., Turner, D. R., and Ahn, T. M. (2001). "Modeling colloid transport for performance assessment." *J Contam Hydrol*, 47, 323–333.

Cromieres, L., Moulin, V., Fourest, B., Guillaumont, R., and Giffaut, E. (1998). "Sorption of thorium onto hematite colloids." *Radiochimica Acta*, 82, 249-255.

Ekberg, C., Albinsson, Y., Comarmond, M. J., and Brown, P. L. (2000). "Studies on the Complexation Behavior of Thorium(IV). 1. Hydrolysis Equilibria." *Journal of Solution Chemistry*, 29(1), 63-86.

Elimelech, M., and Ryan, J. N. (2002). "Interactions between soil particles and Microorganisms: Impact on the Terrestrial Ecosystem."

EPA (2011). "Thorium." Radiation Protection, from http://www.epa.gov/radiation/radionuclides/thorium.html.

EPA (2012). "Plutonium." Radiation Protection, from http://www.epa.gov/radiation/radionuclides/plutonium.html#healtheffects.

Felmy, A. R., Rai, D., Sterner, S. M., Mason, M. J., Hess, N. J., and Conradson, S. D. (1997). "Thermodynamic models for highly charged aqueous species: Solubility of Th(IV) hydrous oxide in concentrated $NaHCO_3$ and Na_2CO_3 solutions." *Journal of Solution Chemistry*, 26(3), 233-248.

Freidman, H. (2011). "The Mineral Thorite." The Mineral & Gemstone Kingdom Retrived Jun. 21, 2011, from http://www.minerals.net/mineral/thorite.aspx.

Gao, B., Saiers, J. E., and Ryan, J. (2006). "Pore-scale mechanisms of colloid deposition and mobilization during steady and transient flow through unsaturated granular media." *Water Resources Research*, 42(1).

Grenthe, I., and B. Lagerman (1991). "Studies on metal carbonate equilibria: 23. Complex formation in the Th(IV)-H_2O-CO_2(g) system." *Acta Chem. Scand.*, 45, 231-238.

Grolimund, D., and M. Borkovec (1999). "Long-term release kinetics of colloidal particles from natural porous media." *Environmental Science & Technology*, 33, 4054–4060.

Grolimund, D., and M. Borkovec (2005). "Colloid-facilitated transport of strongly sorbing contaminants in natural porous media: Mathematical modeling and laboratory column experiments." *Environmental Science & Technology*, 39(17), 6378-6386.

Guo, Z. J., Yu, X. M., Guo, F. H., and Tao, Z. Y. (2005). "Th(IV) adsorption on alumina: Effects of contact time, pH, ionic strength and phosphate." *Journal of Colloid and Interface Science*, 288(1), 51-56.

Haliena, B. (2012). "Chemical Factors Influencing Colloid Mobilization and Th(IV) Transport through Saturated Subsurface Sediment." *Department of Civil Engineering,Auburn, AL, Auburn University*, Masters of Science.

Honeyman, B. D. (1999). "Colloidal culprits in contamination." *Nature*, 397, 23-24.

Hongxia, Z., Jieqiong, Y., and Zuyi, T. (2007). "Effects of phosphate and Cr^{3+} on the sorption and transport of Th(IV) on a silica column." *Journal of Radioanalytical and Nuclear Chemistry*, 273(2), 465-471.

Hongxia, Z., Zheng, D., and Zuyi, T. (2006). "Sorption of thorium(IV) ions on gibbsite: Effects of contact time, pH, ionic Strength, concentration, phosphate and fulvic acid." *Colloids and Surfaces a-Physicochemical and Engineering Aspects*, 278(1-3), 46-52.

Hunter, K. A., Hawke, D. J., and Kwee, C. L. (1988). "Equilibrium adsorption of thorium by metal oxides in marine electrolytes." *Geochimica et Cosmochimica Acta*, 52(3), 627-636.

Jeong, M. S., Y.S., H., and C. H., K. (2011). "Modeling of the pseudo-colloids migration for multi-member decay chains with a arbitrary flux boundary condition in a fractured porous medium." *Radioanalytical & Nuclear Chemistry*, 289(1), 287.

Kanti Sen, T., and Khilar, K. C. (2006). "Review on subsurface colloids and colloid-associated contaminant transport in saturated porous media." *Advances in Colloid and Interface Science*, 119(2-3), 71-96.

Kaplan, D. I., Bertsch, P. M., Adriano, D. C., and Miller, W. P. (1993). "Soil-borne mobile colloids as influenced by water flow and organic carbon." *Environmental Science & Technology*, 27(6), 1193-1200.

Kaplan, D. I., Bertsch, P. M., Adriano, D. C., and Orlandini, K. A. (1994). "Actinide association with groudnwater colloids in a coastal-plain aquifer." *Radiochimica Acta*, 66-7, 181-187.

Kersting, A. B., Efurd, D. W., Finnegan, D. L., Rokop, D. J., Smith, D. K., and Thompson, J. L. (1999). "Migration of plutonium in ground water at the Nevada test site " *Nature*, 397, 56-59.

Khilar, K. C., and Fogler, H. S. (1998). "Migration of Fines in Porous Media.Dor-drecht, Boston, London." *Kluwer Academic Publishers*, Chapter 1,3,9.

Kim, J. I. (1991). "Actinide colloid generation in groundwater." *Radiochimica Acta*, 52-3, 71-81.

Kim, J. S., Kwon, S. K., Sanchez, M., and Cho, G. C. (2011). "Geological Storage of High Level Nuclear Waste." *Ksce Journal of Civil Engineering*, 15(4), 721-737.

Kim, S. S., Baik, M. H., Choi, J. W., Shin, H. S., and Yun, J. I. (2010). "The dissolution of ThO_2(cr) in carbonate solutions and a granitic groundwater." *Journal of Radioanalytical and Nuclear Chemistry*, 286(1), 91-97.

Kretzschmar, R., and Schafer, T. (2005). "Metal retention and transport on colloidal particles in the environment." *Elements*, 1(4), 205-210.

Li, W. J., and Tao, Z. Y. (2002). "Comparative study on Th(IV) sorption on alumina and silica from aqueous solutions." *Journal of Radioanalytical and Nuclear Chemistry*, 254(1), 187-192.

McCarthy, J., and Zachara, J. (1989). "ES&T Features: Subsurface transport of contaminants." *Environmental Science & Technology*, 23(5), 496-502.

McGechan, M. B., and Lewis, D. R. (2002). "Transport of particulate and colloid-sorbed contaminants through soil, part 1: General principles." *Biosystems Engineering*, 83(3), 255-273.

Melson, N. H. (2012). "Sorption of Thorium onto Subsurface Geomedia." *Radiochimica Acta*, 100(11), 827-832.

Milic, N. B. (1981). "Linear Free-Energy Relationships in the Hydrolysis of Metal-Ions - The Effect of the Ionic Medium." *Journal of the Chemical Society-Dalton Transactions*(7), 1445-1449.

Milić, N. B., and Šuranji, T. M. (1982). "Hydrolysis of the thorium(IV) ion in sodium nitrate medium." *Canadian Journal of Chemistry*, 60(11), 1298-1303.

Murphy, R. J., Lenhart, J. J., and Honeyman, B. D. (1999). "The sorption of thorium (IV) and uranium (VI) to hematite in the presence of natural organic matter." *Colloids and Surfaces A: Physicochemical and Engineering Aspects*, 157(1-3), 47-62.

Neck, V., and Kim, J. I. (2001). "Solubility and hydrolysis of tetravalent actinides." *Radiochimica Acta*, 89(1), 1-16.

Neck, V., Müller, R., Bouby, M., Altmaier, M., Rothe, J., Denecke, M. A., and Kim, J.-I. (2002). "Solubility of Amorphous Th(IV) Hydroxide –Application of LIBD to Determine the Solubility Product and EXAFS for Aqueous Speciation." *Radiochimica Acta*, 90(9-11_2002), 485-494.

Nelson, S. A. (2012). "Physical Geology." *Tulane University*(EENS 1110).

Neretnieks, I., and Rasmuson, A. (1984). "An approach to modeling radionuclide migration in a medium with strongly varying velocity and block sizes along the flow path." *Water Resources Research*, 20(12), 1823-1836.

Östhols, E., Bruno, J., and Grenthe, I. (1994). "On The Influence of Carbonate on Mineral Dissolution .3. The Solubility of Microcrystalline ThO_2 in CO_2-H_2O Media." *Geochimica et Cosmochimica Acta*, 58(2), 613-623.

Östhols, E., Manceau, A., Farges, F., and Charlet, L. (1997). "Adsorption of Thorium on Amorphous Silica: An EXAFS Study." *Journal of Colloid and Interface Science*, 194(1), 10-21.

Penrose, W. R., Polzer, W. L., Essington, E. H., Nelson, D. M., and Orlandini, K. A. (1990). "Mobility of plutonium and americium through a shallow aquifer in a semiarid region." *Environmental Science & Technology*, 24(2), 228-234.

Peterson, J., MacDonell, M., Haroun, L., Monette, F., Hildebrand, D., and Taboas, A. (2007). "Radiological and Chemical Fact Sheets to Support Health Risk Analyses for Contaminated Areas, Argonne National Laboratory Environmental Science Division." 133.

Pitts, M. M. (1995). "Fouling mitigation in aqueous systems using electrochemical water treatment.", Retrieved January 24, 2012, From http://www.zetacorp.com/fouling_mitigation.shtml.

Prasad, R., Beasley, M. L., and Milligan, W. O. (1967). "Aging of Hydrous Thoria Gels." *Journal of Electron Microscopy*, 16(2), 101-119.

Priesing, C. P. (1962). "A theory of coagulation useful for design." *Industrial & Engineering Chemistry*, 54(8), 38-45.

Pshinko, G., Timoshenko, T., and Bogolepov, A. (2009). "Effect of fulvic acids on Th(IV) sorption on montmorillonite." *Radiochemistry*, 51(1), 91-95.

Rai, D., Moore, D. A., Oakes, C. S., and Yui, M. (2000). "Thermodynamic model for the solubility of thorium dioxide in the Na^{+}-Cl--OH--H_2O system at 23 degrees C and 90 degrees C." *Radiochimica Acta*, 88(5), 297-306.

Rand, M., Fuger, J., Neck, V., Grenthe, I., and Rai, D. (2008). *Chemical Thermodynamics of Thorium*, North Holland Elsevier Science Publishers B. V, Amsterdam, The Netherlands.

Reiller, P., Moulin, V., Casanova, F., and Dautel, C. (2002). "Retention behaviour of humic substances onto mineral surfaces and consequences upon thorium (IV) mobility: case of iron oxides." *Applied Geochemistry*, 17(12), 1551-1562.

Rojo, I., Seco, F., Rovira, M., Giménez, J., Cervantes, G., Martí, V., and Pablo, J. d. (2009). "Thorium sorption onto magnetite and ferrihydrite in acidic conditions." *Journal of Nuclear Materials*, 385(2), 474-478.

Runde, W. (2000). "The Chemical Interactions of Actinides in the Environment." *Los Alamos Science*, 26, 392-411.

Ryan, J. L., and Rai, D. (1987). "Thorium(IV) Hydrous Oxide Solubility." *Inorganic Chemistry*, 26(24), 4140-4142.

Ryan, J. N., and Elimelech, M. (1996). "Colloid mobilization and transport in groundwater." *Colloids and Surfaces a-Physicochemical and Engineering Aspects*, 107, 1-56.

Ryan, J. N., Illangasekare, T. H., Litaor, M. I., and Shannon, R. (1998). "Particle and plutonium mobilization in macroporous soils during rainfall simulations." *Environmental Science & Technology*, 32(4), 476-482.

Saiers, J. E., and Hornberger, G. M. (1996). "The role of colloidal kaolinite in the transport of cesium through laboratory sand columns." *Water Resour. Res*, 32, 33-41.

Saiers, J. E., and Hornberger, G. M. (1999). "The influence of ionic strength on the facilitated transport of cesium by kaolinite colloids." *Water Resources Research*, 35, 1713-1727.

Saiers, J. E., and Lenhart, J. J. (2003). "Colloid mobilization and transport within unsaturated porous media under transient-flow conditions." *Water Resources Research*, 39(1).

Sardin, M., Schweich, D., Leij, F. J., and Vangenuchten, M. T. (1991). "Modeling the non-equilibrium transport of lineraly interacting solutes in porous media: A Review." *Water Resources Research*, 27(9), 2287-2307.

Satterfield, Z. (2005). "Jar Testing." *Tech Brief*, 5(1), From http://www.nesc.wvu.edu/pdf/dw/publications/ontap/2009_tb/jar_testing_dwfsom2073.pdf.

Seaborg, G. T., and Loveland, W. D. (1990). "The Elements Beyond Uranium." *Wiley Interscience*, New York.

Seco, F., Hennig, C., Pablo, J. D., Rovira, M., Rojo, I., Mart ί V., Gimenez, J., Duro, L., M.Grive, and Bruno, J. (2009). "Sorption of Th(IV) onto Iron Corrosion Products: EXAFS Study." *Environmental Science & Technology*, 43(8), 2825-2830.

Sen, T. K., and Khilar, K. C. (2006). "Review on subsurface colloids and colloid-associated contaminant transport in saturated porous media." *Advances in Colloid and Interface Science*, 119(2-3), 71-96.

Sen, T. K., Mahajan, S. P., and Khilar, K. C. (2002). "Colloid-associated contaminant transport in porous media: 1. Experimental studies." *AIChE*, 48(10), 2366-2374.

Sharma, M. M., Chamoun, H., Sarma, D. S. H. S. R., and Schechter, R. S. (1992). "Factors controlling the hydrodynamic detachment of particles from surfaces." *ournal of Colloid and Interface Science*, 149(1), 121-134.

Snoeyink, V. L., and Jenkins, D. (1980). *Water chemistry*.

Sprague, L. A., Herman, J. S., Hornberger, G. M., and Mills, A. L. (2000). "Atrazine adsorption and colloid-facilitated transport through the unsaturated zone." *Journal of Environmental Quality*, 29(5), 1632-1641.

Stumm, W. (1977). "Chemical interaction in particle separation." *Environmental Science & Technology*, 11(1066–1070.).

Sun, H., Gao, B., Tian, Y., Yin, X., Yu, C., Wang, Y., and Ma, L. Q. (2010). "Kaolinite and Lead in Saturated Porous Media: Facilitated and Impeded Transport." *ENVIRONMENTAL ENGINEERING*, 136(11), 1305-1308.

Šuranji, T. M., and Milić, N. B. (1981). "Hydrolysis of thorium(IV) ions in lithium and potassium chloride media." *Glas. Hem. Drus. Beograd*, 46, 657-661.

Tan, X., Wang, X., Chen, C., and Sun, A. (2007). "Effect of soil humic and fulvic acids, pH and ionic strength on Th(IV) sorption to TiO_2 nanoparticles." *Applied Radiation and Isotopes*, 65(4), 375-381.

Zhao, D. L., Feng, S. J., Chen, C. L., Chen, S. H., Xu, D., and Wang, X. K. (2008). "Adsorption of thorium(IV) on MX-80 bentonite: Effect of pH, ionic strength and temperature." *Applied Clay Science*, 41(1-2), 17-23.

Zhijun, G., Lijun, N., and Zuyi, T. (2005). "Sorption of Th(IV) ions onto TiO_2: Effects of contact time, ionic strength, thorium concentration and phosphate." *Journal of Radioanalytical and Nuclear Chemistry*, 266(2), 333-338.

Zhu, Y., Ma, L. Q., B.Gao, Bonzongo, J. C., W.Harris, and Gu, B. (2012). "Transport and interactions of kaolinite and mercury in saturated sand media." *Journal of Hazardous Materials*, 213-214, 93-99.

Appendices

Appendix A. Column Characteristics and Setup

Table A.1: Column transport experiment characteristics

Column ID	Exp#1	Exp#2	Exp#3	Exp#4	Exp#5	Exp#6	Exp#7	Exp#8	Exp#9
Height (cm)	12.20	12.10	12.05	12.05	12.10	12.05	12.00	12.10	12.10
Diameter(cm)	2.5	2.5	2.5	2.5	2.5	2.5	2.5	2.5	2.5
Mass of Pure Quartz Sands (g)	94.02	94.08	93.30	92.84	93.67	92.75	92.00	93.97	93.50
Total Column Volume V_t(mL)	59.89	59.40	59.15	59.15	59.40	59.15	58.90	59.40	59.40
Specific Discharge q (cm/min)	0.2	0.2	0.2	0.2	0.2	0.2	0.2	0.2	0.2
Bulk Density ρ_b (g/cm^3)	1.57	1.58	1.58	1.57	1.58	1.57	1.56	1.58	1.57
Porosity ϕ	0.408	0.402	0.405	0.408	0.405	0.408	0.411	0.403	0.406
Soil Pore Volume V_0 (mL)	24.41	23.89	23.94	24.12	24.05	24.15	24.19	23.94	24.11
Retention Time θ (min)	24.41	23.89	23.94	24.12	24.05	24.15	24.19	23.94	24.11
Th(IV) Influent Concentration (mg/L)	N/A	0.93	2.66	0.97	2.65	0.99	2.62	0.99	2.68
Th(IV) Influent Concentration (M)	N/A	4.01E-06	1.15E-05	4.18E-06	1.14E-05	4.27E-06	1.13E-05	4.27E-06	1.16E-05
Dispersion Coefficient D (cm^2/min)	0.03	-	0.03	0.03	0.04	-	-	-	-
Column Peclet Number N_{pe}	224.59	-	203.39	171.44	170.04	-	-	-	-

Note: (1) " –" means this option did not perform

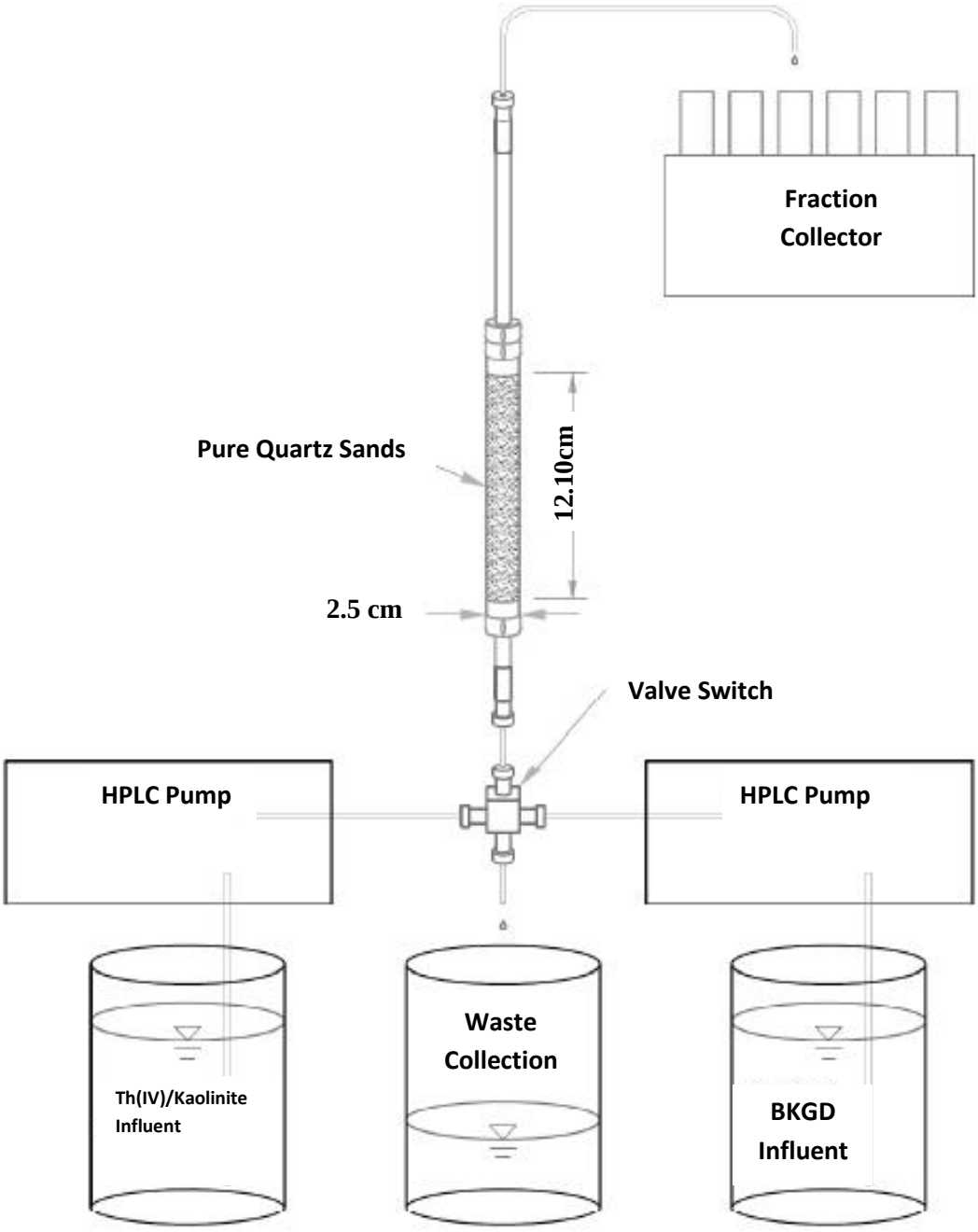

Figure A.1 Schematic of the Laboratory Column Transport Experiment Setup, adapted from Haliena (2012). BKGD indicates background solution.

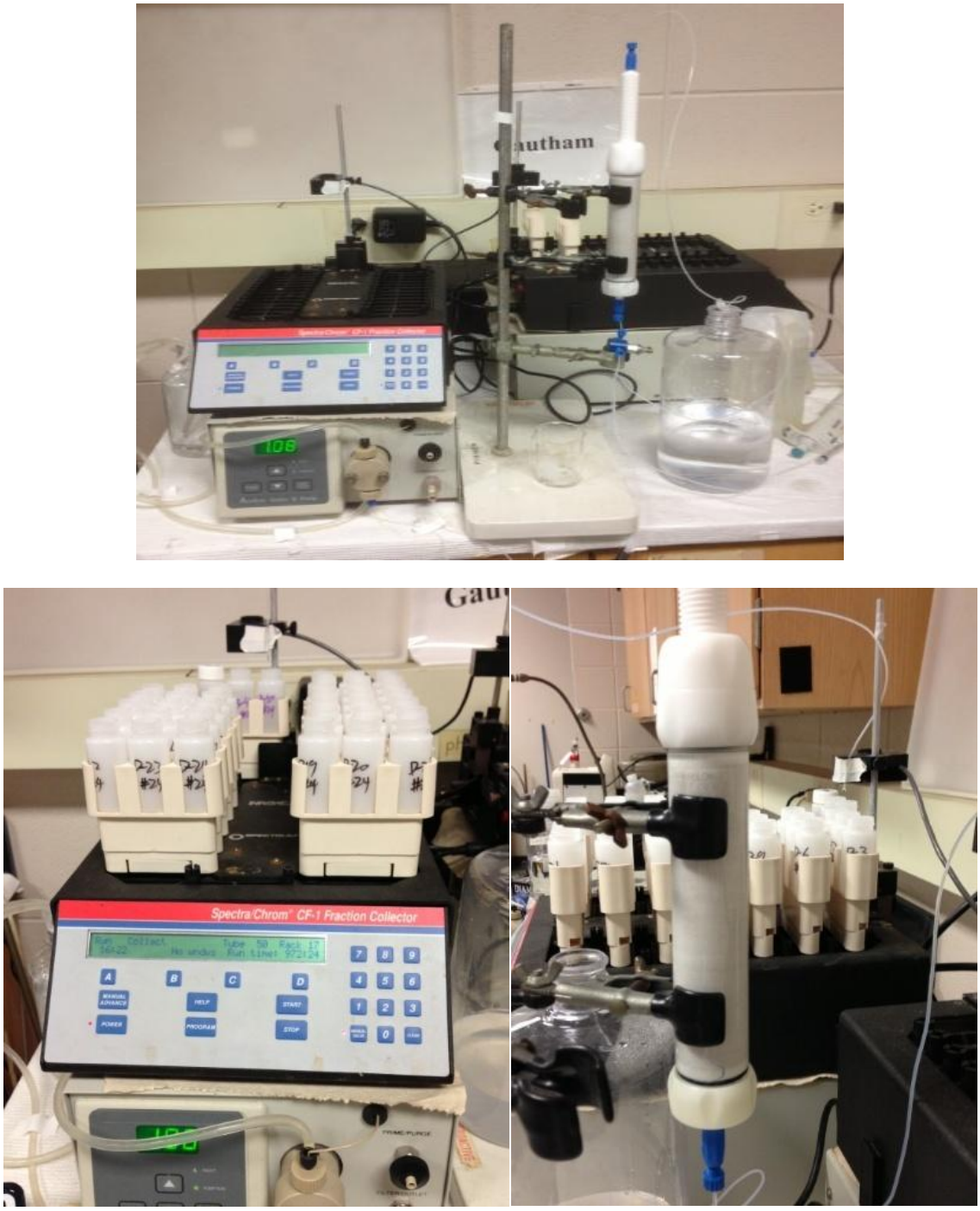

Figure A.2: Images of experiment setup (Omnifit glass column packed with pure quartz sands).

Appendix B. Colloidal Kaolinite Concentration Calibration Curves and Bromide Tracer Test

The following calibration curves were used to correlate measured effluent turbidity to kaolinite concentration. The calibration curves were produced by measuring the turbidity and kaolinite concentration (by gravimetric analysis)

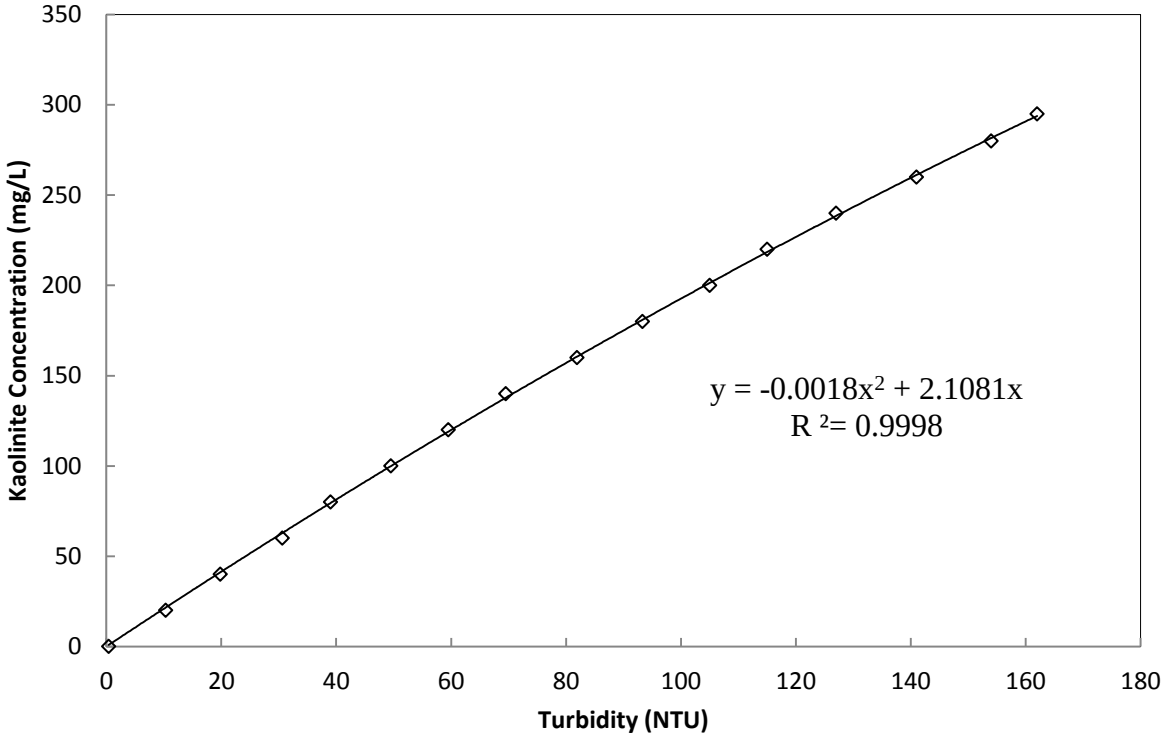

Figure B.1: Correlation curve between colloid concentrations and turbidity under the condition of 0.001M ionic strength at a pH of 4.0.

The Following bromide tracer breakthrough curve was fitted with CXTFIT to determine the hydrodynamic properties of the column.

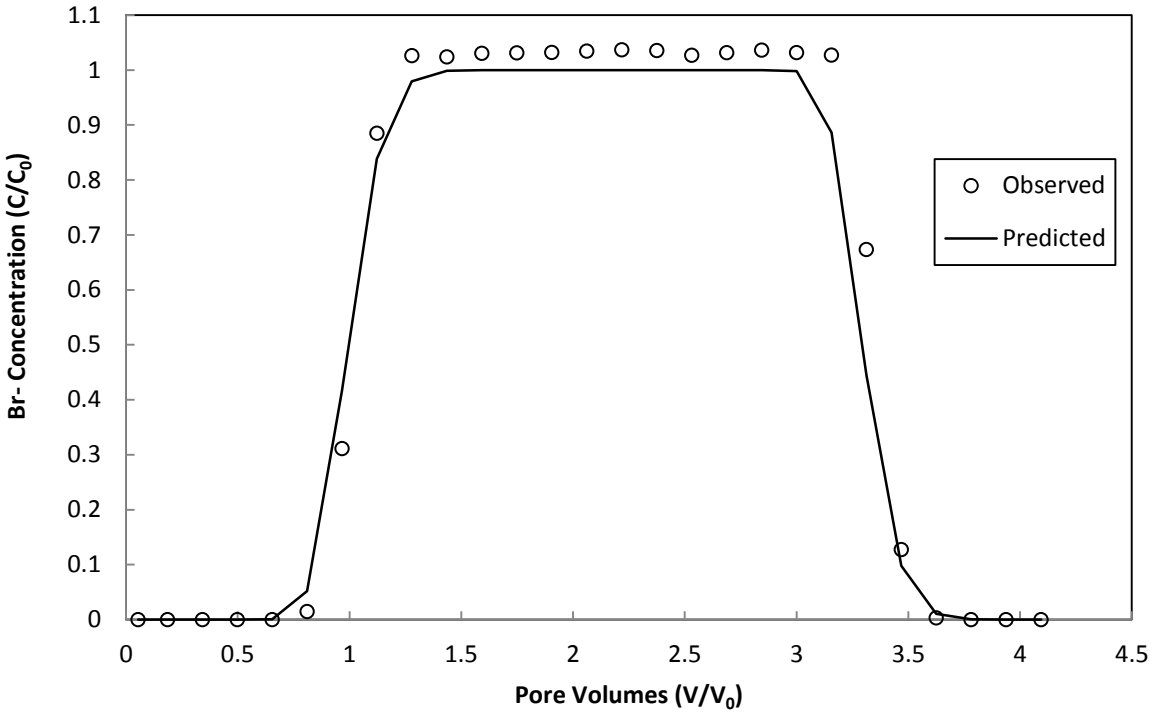

Figure B.2: Exp#4 Br- tracer breakthrough curve fitted with CXTFIT (C_0=48.6 mg/L, q=0.2 cm/min, λ=0.07 cm, R^2=0.98, D=0.03 cm^2/min, N_{pe}=171.44).

Appendix C. Sample Calculations

The following calculations were used to determine the results shown in chapter 3.

1.) <u>Total empty column volume, V_t</u>

Equation: $V_t = \pi \cdot \left(\frac{d}{2}\right)^2 \cdot H$

Where: V_t = Total empty column volume (cm^3),
d = Inside diameter of column (cm), and
H = Height of soil inside column (cm)

Example: Column Exp#4

Given: d=2.5cm, H=12.05cm

$V_t = \pi \cdot \left(\frac{2.5cm}{2}\right)^2 \cdot 12.05cm$ =59.15 cm^3

2.) <u>Specific discharge, q</u>

Equation: $q = \frac{Q}{A} = \frac{Q}{\pi(\frac{d}{2})^2}$

Where: q = Specific discharge (cm/min),
Q = Pump flow rate (cm^3/min),
A = Cross sectional area of column (cm^2), and
d = Inside diameter of column (cm)

Example: Column Exp #4

Given: Q = 1 mL/min, d = 2.5 cm

$$q = \frac{Q}{A} = \frac{1ml/min}{\pi(\frac{2.5cm}{2})^2} = 0.20cm/min$$

3.) <u>Bulk density, ρ_b</u>

Equation: $\rho_b = \frac{m}{V_t}$

Where: ρ_b = Bulk density (g/cm^3),
m = Dry packed soil mass (g), and
V_t = Total empty column volume (cm^3)

Example: Column Exp #4

Given: m = 92.84 g, V_t = 59.15 cm^3

$$\rho_b = \frac{92.8g}{59.15cm^3} = 1.57\frac{g}{cm^3}$$

4.) <u>Porosity, φ</u>

Equation: $\varphi = 1 - \frac{\rho_b}{\rho_p}$

Where: φ = Porosity,
ρ_b = Bulk density (g/cm^3), and
ρ_p = Particle density (assume quartz = 2.65 g/cm^3)

Example: Column Exp #4

Given: ρ_b = 1.57 g/cm^3, ρ_p = 2.65 g/cm^3

$$\varphi = 1 - \frac{1.57\frac{\text{g}}{\text{cm}^3}}{2.65\frac{\text{g}}{\text{cm}^3}} = 0.408$$

5.) <u>Column pore volume, V_0</u>

Equation: $V_0=V_t\varphi$

Where: V_0 = Column pore volume (mL)
V_t = Total empty column volume (mL), and
φ = Porosity

Example: Column Exp #4

Given: V_t = 59.15 cm^3, φ = 0.408

V_0=59.15 cm^3 (0.408) = 24.12 cm^3

6.) <u>Pore water velocity, v</u>

Equation: $\nu = \frac{Q}{A \cdot \varphi} = \frac{Q}{\pi \cdot (\frac{d}{2})^2 \cdot \varphi}$

Where: ν = Average flow velocity (cm/min),
Q = Pump flow rate (cm^3/min),
A = Cross sectional area of column (cm^2),
d = Inside diameter of column (cm), and
φ = Porosity

Example: Column Exp #4

Given: Q = 1 cm^3/min, d = 2.5 cm, φ = 0.408

$\nu = \frac{Q}{A \cdot \varphi} = \frac{1\frac{cm^3}{min}}{\pi \cdot (\frac{2.5cm}{2})^2 \cdot 0.408}$ =0.5 cm/min

7.) Retention Time, θ

Equation: $\theta = \frac{H}{v} = \frac{V_0}{Q}$

Where: H = Height of soil inside column (cm),
v = Average flow velocity (cm/min),
V_0 = Column pore volume (cm^3), and
Q = Pump flow rate (cm^3/min)

Example: Column Exp #4
Given: H = 12.05 cm, v = 0.5 cm/min, V_0 = 24.12 mL, Q = 1 cm^3/min

$\theta = \frac{H}{v} = \frac{12.05cm}{0.5cm/min} = 24.10 \text{ min } or\ \theta = \frac{V_0}{Q} = \frac{24.12mL}{1\frac{cm^3}{min}} = 24.12min$

8.) Dispersion Coefficient, D

Equation: $D = \lambda \cdot v$

Where: D = Dispersion coefficient (cm^2/min),
λ = Dispersivity coefficient from Br- tracer test (cm), and
v = Average flow velocity (cm/min)

Example: Column Exp #4

Given: λ=0.07 cm, v = 0.5cm/min

D=0.07cm 0.5 cm/min= 0.035cm^2/min

9.) Peclet Number, N_{pe}

Equation: $N_{pe} = \frac{H \cdot v}{D}$

Where: H = Height of soil inside column (cm)
v = Average flow velocity (cm/min)
D = Dispersion coefficient (cm^2/min), and

Example: Column Exp #4
Given: H = 12.05cm, v = 0.5 cm/min, D = 0.035 cm^2/min

$N_{pe} = \frac{12.05cm \cdot 0.5cm/min}{0.035cm^2/min}$=172.14

10.) **Percent Recovery**

Equation: $\%\ \text{Recovery} = \frac{\text{Mass}_{\text{adsorbed}} + \text{Mass}_{\text{desorbed}}}{\text{Mass}_{\text{in}}} \cdot 100$

Where: $\text{Mass}_{\text{adsorbed}}$ = Cumulative mass of Th(IV) in the effluent solutions during the sorption phase calculated by trapezoidal rule,

$\text{Mass}_{\text{desorbed}}$ = Cumulative mass of Th(IV) in the effluent solutions during the desorption phase calculated by trapezoidal rule, and

Mass_{in} = Cumulative mass of Th(IV) introduced to the column in the influent solution during the sorption phase

Example: Column Exp #1

Given: Average kaolinite influent concentration, C_0 = 99.4 mg/L; cumulative volume of the influent Th(IV) solution introduced to the column, V = 179.786 mL; kaolinite concentrations in effluent samples, C_i (mg/L); cumulative volume of effluent samples, V_i (mL)

$$\%\ \text{Recovery} = \frac{\text{Mass}_{\text{adsorbed}} + \text{Mass}_{\text{desorbed}}}{\text{Mass}_{\text{in}}} \cdot 100 = \frac{13.5733\text{mg} + 2.2068\text{mg}}{99.4\text{mg/L} \cdot 179.786\text{mL}} = 88\%$$

Appendix D. Pictures for the Process of Jar Testing

The following pictures visually demonstrated the processes and results of the jar testing

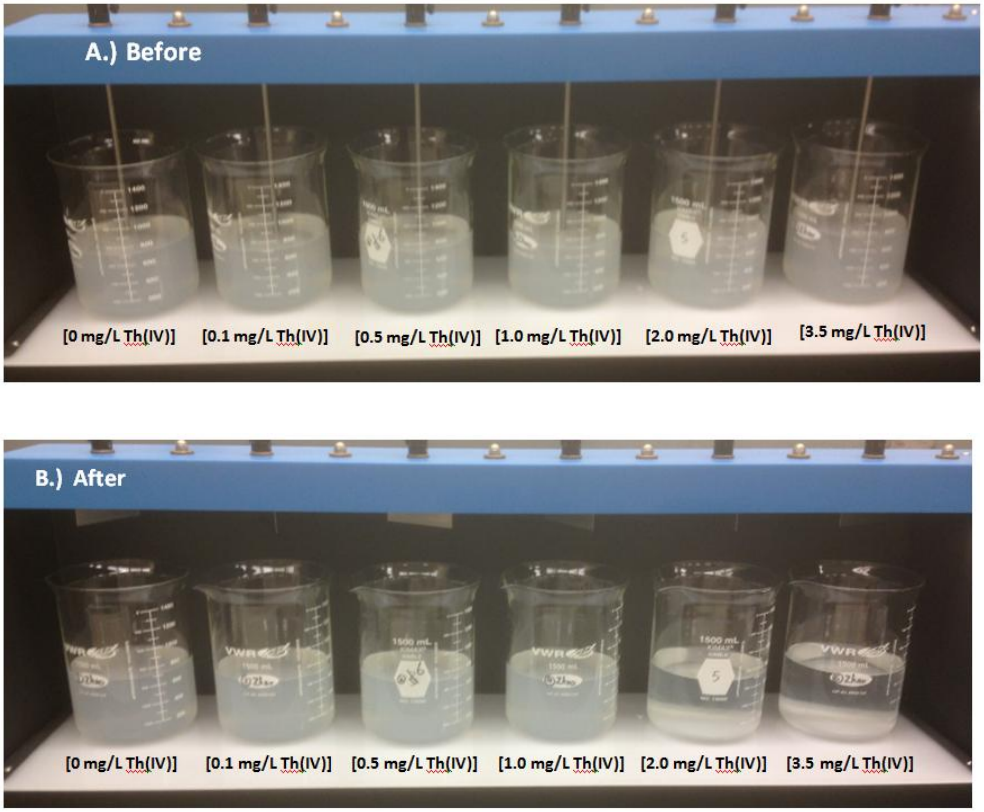

Figure D.1: Pictures for the process of Jar Test in which turbidity was caused by 100 mg/L kaolinite. Picture A is before stirring, and picture B is after stirring and 30 mins standing.